J. Phys. G: Nucl. Part. Phys. **26** (2000) 551–591. Printed in the UK PII: S0954-3899(00)11789-X

Report of the 'Beyond the Standard Model' working group of the 1999 UK Phenomenology Workshop on Collider Physics (Durham)

B C Allanach[1]†, J J van der Bij[2], A Dedes[3], A Djouadi[4], J Grosse-Knetter[5], J Hetherington[6], S Heinemeyer[7], J Holt[5], D Hutchcroft[8], J Kalinowski[9], G Kane[10], V Kartvelishvili[11], S F King[12], S Lola[13]†, R McNulty[14], M A Parker[6], G D Patel[14], G G Ross[15], M Spira[16], P Teixeira-Dias[17], G Weiglein[13], G Wilson[11], J Womersley[18], P Walker[11], B R Webber[6] and T Wyatt[11]†

[1] DAMTP, Silver Street, University of Cambridge, Cambridge CB3 9EW, UK
[2] Fakultaet fuer Physik, Universitaet Freiburg, H Herderstr. 3, 79104 Freiburg i. B., Germany
[3] Rutherford Appleton Laboratory, Chilton, Didcot, Oxon OX11 OQX, UK
[4] Laboratoire de Physique Mathématique et Théorique, UMR–CNRS 5825, Université de Montpellier II, F-34095 Montpellier Cedex 5, France
[5] Nuclear Physics Laboratory, University of Oxford, Keble Road, Oxford OX1 3RH, UK
[6] Cavendish Laboratory, University of Cambridge, Madingley Road, Cambridge CB3 OHE, UK
[7] Deutsches Elektronen Synchrotron (DESY), Notkestrasse 85, D-22603 Hamburg, Germany
[8] Physics Department, Royal Holloway University of London, Egham Hill, Egham, Surrey TW20 0EX, UK
[9] Instytut Fizyki Teoretycznej UW, Hoza 69, PL-00681 Warsaw, Poland
[10] Randall Physics Laboratory, University of Michigan, Ann Arbor, MI 48109-1120, USA
[11] Department of Physics and Astronomy, Schuster Laboratory, The University of Manchester, Manchester M13 9PL, UK
[12] Department of Physics and Astronomy, University of Southampton, Highfield, Southampton SO17 1BJ, UK
[13] Theory Division, CERN, CH-1211 Geneva 23, Switzerland
[14] Department of Physics, Oliver Lodge Laboratory, University of Liverpool, PO Box 147, Oxford Street, Liverpool L69 3BX, UK
[15] Department of Theoretical Physics, University of Oxford, 1 Keble Road, Oxford OX1 3NP, UK
[16] Institut fur Theoretische Physik, Universitat Hamburg, Luruper Chaussee 149, D-22761 Hamburg, Germany
[17] Department of Physics and Astronomy, University of Glasgow, Kelvin Building, Glasgow G12 8QQ, UK
[18] Fermilab, PO Box 500, Batavia, IL 60510-0500, USA

Received 8 February 2000

Abstract. The 'Beyond the Standard Model' working group discussed a variety of topics relating to exotic searches at current and future colliders, and the phenomenology of current models beyond the standard model (SM). For example, various supersymmetric (SUSY) and extra dimensions search possibilities and constraints are presented. Fine-tuning implications of SUSY searches are derived. The implications of Higgs (non)discovery are discussed, as well as the program HDECAY. The individual contributions are included separately. Much of the enclosed work is original, although some is reviewed.

(Some figures in this article are in colour only in the electronic version; see `www.iop.org`)

† Convenors.

1. Introduction

The 'Beyond the Standard Model' working group addressed the prospects for searches for supersymmetry (SUSY), the phenomenology of large extra dimensions and the phenomenological implications of lower bounds upon the Higgs boson mass. The present status of large extra dimensions, SUSY breaking and searches for SUSY and leptoquarks were well covered in the plenary talks by G Ross and J Womersley.

There were three broad subgroups: Higgs phenomenology, SUSY breaking/large extra dimensions and the study of events containing isolated charged leptons and missing p_t at LEP2. These subgroups had their own agendas of seminar presentations, discussions and reports. Summaries from each subgroup were given to the rest of the 'Beyond the Standard Model' working group, and indeed the other working groups of the workshop. Much of the following work is original and carried out at the workshop, whereas some is the result of literature reviews.

The minimal supergravity (mSUGRA) reach potential of the LHC is readdressed in section 2. The exclusion limits are produced in terms of a naturalness parameter. In section 3, the fine-tuning implications of SUSY particle masses are presented in various SUSY-breaking scenarios. The possibilities of detecting gluino–gluino bound states at run II of the Tevatron are examined in section 4. The experimental signatures and fits to current data of two models of extra dimensions are presented in section 5. In section 6, events containing isolated leptons and missing p_t at LEP2 are discussed as a means of detecting, e.g., single chargino and $\tilde{e}_L^+\tilde{e}_R^-$ production. Lower bounds upon the Higgs mass from LEP2 have been steadily increasing in the last two years, and the next sections address this empirical information. We present a review of what the precision electroweak fits imply once one retreats from the SM Higgs sector in section 7. Stealthy Higgs models that may be undetectable by the LHC are reviewed in section 8. State-of-the-art upper limits upon the lightest Higgs boson mass in the general (R-parity conserving) MSSM and mSUGRA are presented in section 9. Within the MSSM, using the most recent and prospective future LEP2 data, limits on $\tan\beta$ are derived. Continuing work upon the Higgs decay program HDECAY was carried out at the workshop and the program is reviewed in section 10.

Acknowledgments

Many thanks to St John's College, Durham where the workshop was held, to M Whalley, J Forshaw and E W N Glover for their organization. This work is partially supported by PPARC.

2. Naturalness reach of the large hadron collider in mSUGRA

B C Allanach, J P J Hetherington, M A Parker, G G Ross and B R Webber

Abstract. We re-analyse the best supergravity (SUGRA) discovery channel at the LHC, in order to re-express coverage in terms of a fine-tuning parameter and to extend the analysis to higher $m_0 = 3$ TeV. Such high values of m_0 have recently been found to have a focus point, leading to relatively low fine-tuning. It is found that even for m_0 as high as 3 TeV, mSUGRA can still be discovered for $M_{\frac{1}{2}} < 490 \pm 20$ GeV. For $\mu < 0$, $A_0 = 0$ GeV and $\tan\beta = 10$ (corresponding to the focus point), all points in mSUGRA with a fine-tuning measure up to 220 are covered by the search.

Recent work [1] has shown that MSSM scalar masses as large as 2–3 TeV can be consistent with naturalness. This occurs near a 'focus point' where the renormalization group (RG) trajectories of the mass squared of a Higgs doublet ($m^2_{\mathrm{H}_2}$) cross close to the electroweak scale. As a result, the electroweak symmetry breaking is insensitive to ultraviolet boundary conditions upon SUSY-breaking parameters [1]. Previous predictions of the discovery reach of the LHC into mSUGRA parameter space went only as far as $m_0 < 2$ TeV [2]. The purpose of this work is to extend this reach to 3 TeV and to present it in terms of a naturalness measure. While interpretation of a naturalness measure is inevitably subjective, we advocate its use as a single parameter for defining the search reach of a collider in the context of a particular model. The naturalness coverage could then be used to compare between different colliders/experiments/models etc.

At tree level, the Z-boson mass is determined to be

$$\tfrac{1}{2}M_{\mathrm{Z}}^2 = \frac{m^2_{\mathrm{H}_1} - m^2_{\mathrm{H}_2}\tan^2\beta}{\tan^2\beta - 1} - \mu^2 \tag{1}$$

by minimizing the Higgs potential, where $\tan\beta$ refers to the ratio of Higgs vacuum expectation values (VEVs) v_1/v_2 and μ to the Higgs mass parameter in the MSSM superpotential. In mSUGRA, m_{H_2} has the same origin as the superpartner masses (m_0). Thus, as search limits put lower bounds upon superpartners' masses, the lower bound upon m_0 rises, and consequently so does $|m_{\mathrm{H}_2}|$. A cancellation is then required between the first and second terms of equation (1) in order to provide the measured value of $M_{\mathrm{Z}} \ll |m_{\mathrm{H}_2}|$. Various measures have been proposed in order to quantify this cancellation [4].

The definition of naturalness c_a of a 'fundamental' parameter a employed in [1] is

$$c_a \equiv \left| \frac{\partial \ln M_{\mathrm{Z}}^2}{\partial \ln a} \right|. \tag{2}$$

From a choice of a set of fundamental parameters $\{a_i\}$, the fine-tuning of a particular model is defined to be $c = \max(c_a)$. Our choice of free, continuously valued, independent and fundamental mSUGRA parameters also follows [1]:

$$\{a_i\} = \{m_0, M_{1/2}, \mu(M_{\mathrm{GUT}}), A_0, B(M_{\mathrm{GUT}})\} \tag{3}$$

where $M_{\mathrm{GUT}} \sim 10^{16}$ GeV is the GUT scale.

We now turn to the discussion of the LHC mSUGRA search. In the ATLAS TDR [2] the best reach was found through a one lepton plus jets plus missing transverse momentum signal, which looks mainly for chargino decays to lepton and sneutrino. The following cuts were employed, which are the same as those as in [2, 3] except where those original cuts are included in parenthesis:

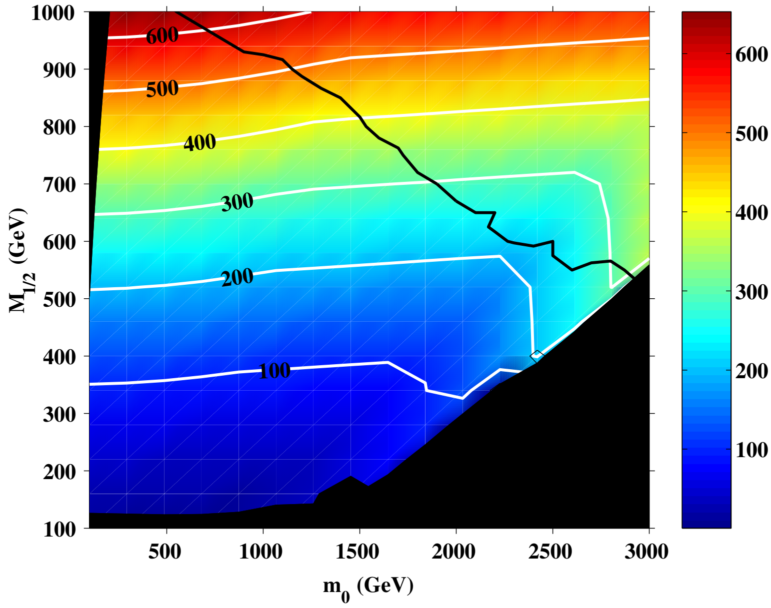

Figure 1. Naturalness reach at the LHC for $A_0 = 0$ GeV, $\tan\beta = 10$, $\mu < 0$ in mSUGRA. The background represents the degree of fine-tuning c, as measured by the bar and white contours. The black region in the top left-hand corner is excluded by the requirement that the LSP be neutral, and the black region at the bottom of the plot from chargino exclusion limits and radiative symmetry breaking. The black curve is the LHC expectation contour for ten signal events in the one-lepton two-jets channel described in the text for a luminosity of $\mathcal{L} = 10$ fb^{-1}.

- $\not{p}_T > 400$ GeV
- At least two jets, with rapidity $\eta < 2.0$, and $p_T > 400$ GeV.
- One lepton, $\eta < 2.0$, $p_T > 20$ GeV, lying further in η, ϕ space than 0.4 units from the centre of any jet with cone size 0.4 (0.7) (less than 5 GeV of energy within 0.3 units of the lepton).
- $$M_T = \sqrt{2(|\boldsymbol{p}_l||\not{\boldsymbol{p}}_T| - \boldsymbol{p}_l \cdot \not{\boldsymbol{p}}_T} > 100 \text{ GeV}, \tag{4}$$
  where $\boldsymbol{p}_l$, $\not{\boldsymbol{p}}_T$ are transverse two-component lepton and missing p_T respectively.
- $$S_T = \frac{2\lambda_2}{\lambda_1 + \lambda_2} > 0.2, \tag{5}$$
  where λ_i are the eigenvalues of the sphericity matrix $S_{ij} = \Sigma_{ij} p_i p_j$, the sum being taken over all detectable final-state particles, and p_i being the two-component transverse momentum attributed to the cell.

mSUGRA events were simulated by employing the ISASUSY part of the ISAJET7.42 package [5] to calculate sparticle masses and branching ratios, and HERWIG6.1 [6] to simulate the events themselves. Figure 1 shows the contour for ten signal events passing the above cuts as a black curve in the $m_0/M_{1/2}$ plane for mSUGRA with $A_0 = 0$ GeV, $\tan\beta = 10$, $m_t(m_t) = 160$ GeV, $\mu < 0$ and for $\mathcal{L} = 10$ fb^{-1} of luminosity (equivalent to one year of running in the low-luminosity mode). Background at regions of parameter space with such high-energy cuts is estimated to be negligible. The discovery contour is overlaid upon the density of naturalness c (displayed as background) as defined above. c was calculated numerically to one-loop accuracy in soft masses, with two-loop accuracy in SUSY parameters and step-function decoupling of sparticles. Dominant one-loop top/stop corrections are added to the Higgs potential and correct equation (1). This approximation was also used to calculate the black (excluded) regions in figure 1. Note that the horizontal piece of the bottom black region results from the limit $M_{\chi_1^\pm} > 90$ GeV, whereas the diagonal piece is from the constraint of electroweak symmetry breaking. This last constraint is very sensitive to $m_t(m_t)$, and moves to the right and off the plot for $m_t(m_t) = 165$ GeV. Note that while the naturalness contours displayed in figure 1 are of the same shape as those calculated before [1], the fine-tuning is some 50% higher. This is due (see, for example, [4]) to the approximation of using an incomplete one-loop potential, and will be rectified [7] (as will the approximation of using constant $m_t(m_t)$ over the $M_{1/2}/m_0$ plane).

Acknowledgments

Part of this work was produced using the Cambridge University High Performance Computing Facility. BCA would like to thank K Matchev for valuable discussions on checking of the numerical results. JH would like to thank C Lester for useful discussions.

References

[1] Feng J L *et al* 2000 *Phys. Rev.* D **61** 075005
Feng J L *et al* 1999 *Preprint* hep-ph/9908309
[2] ATLAS Collaboration 1999 *Detector and Physics Performance TDR* vol 2 *Technical Report* CERN/LHCC 99-15
[3] Baer H *et al* 1996 *Phys. Rev.* D **53** 6241
[4] Barbieri R and Strumia A 1998 *Phys. Lett.* B **433** 63
de Carlos B and Casas J A 1993 *Phys. Lett.* B **320** 320
[5] Baer H *et al* 1998 *Preprint* hep-ph/9810440
[6] HERWIG6.1 collaboration http://home.cern.ch/∼seymour/herwig/herwig61.html
(HERWIG6.1 collaboration 1999 *Preprint* Cavendish-HEP-99/03)
[7] Allanach B C *et al* work in progress

3. Fine-tuning constraints on SUGRA models

M Bastero-Gil, G L Kane and S F King

Abstract. We discuss fine-tuning constraints on SUGRA models. The tightest constraints come from the experimental mass limits on two key particles: the lightest CP-even Higgs boson and the gluino. We also include the lightest chargino which is relevant when universal gaugino masses are assumed. For each of these particles we show how fine-tuning increases with the experimental mass limit, for four types of SUGRA model: mSUGRA, no-scale SUGRA (relaxing the universal gaugino mass assumption), D-brane models and anomaly-mediated SUSY-breaking models. Among these models, the D-brane model is less fine-tuned. The experimental prospects for an early discovery of Higgs and SUSY at LEP and the Tevatron are discussed in this framework.

When should physicists give up on low-energy SUSY? The question revolves around the issue of how much fine-tuning one is prepared to tolerate. Although fine-tuning is not a well defined concept, the general notion of fine-tuning is unavoidable since it is the existence of fine-tuning in the standard model (SM) which provides the strongest motivation for low-energy SUSY, and the widespread belief that superpartners should be found before or at the LHC. Although a precise measure of *absolute* fine-tuning is impossible, the idea of *relative fine-tuning* can be helpful in selecting certain models and regions of parameter space over others†.

The models we consider, and the corresponding input parameters given at the unification scale, are listed below:

(i) mSUGRA

$$a_{\rm mSUGRA} \in \{m_0^2, M_{1/2}, A(0), B(0), \mu(0)\}, \tag{6}$$

where as usual m_0, $M_{1/2}$ and $A(0)$ are the universal scalar mass, gaugino mass and trilinear coupling respectively, $B(0)$ is the soft breaking bilinear coupling in the Higgs potential and $\mu(0)$ is the Higgsino mass parameter.

(ii) No-scale SUGRA with non-universal gaugino masses‡

$$a_{\text{no-scale}} \in \{M_1(0), M_2(0), M_3(0), B(0), \mu(0)\}. \tag{7}$$

(iii) The D-brane model

$$a_{\text{D-brane}} \in \{m_{3/2}, \theta, \Theta_1, \Theta_2, \Theta_3, B(0), \mu(0)\}, \tag{8}$$

where θ and Θ_i are the goldstino angles, with $\Theta_1^2+\Theta_2^2+\Theta_3^2 = 1$, and $m_{3/2}$ is the gravitino mass. The gaugino masses are given by

$$\begin{aligned} M_1(0) &= M_3(0) = \sqrt{3} m_{3/2} \cos\theta \Theta_1 \mathrm{e}^{-\mathrm{i}\alpha_1}, \\ M_2(0) &= \sqrt{3} m_{3/2} \cos\theta \Theta_2 \mathrm{e}^{-\mathrm{i}\alpha_2}, \end{aligned} \tag{9}$$

and there are two types of soft scalar masses:

$$\begin{aligned} m_{5152}^2 &= m_{3/2}^2[1 - \tfrac{3}{2}(\sin^2\theta + \cos^2\theta\Theta_3^2)], \\ m_{51}^2 &= m_{3/2}^2[1 - 3\sin^2\theta]. \end{aligned} \tag{10}$$

† For a complete list of references and a fuller discussion of these results see [1].

‡ This is in fact a new model not previously considered in the literature, although the no-scale model with universal gaugino masses is of course well known. As in the usual no-scale model, this model has the attractive feature that flavour-changing neutral currents (NCs) at low energies are very suppressed, since all the scalar masses are generated by radiative corrections, via the RG equations, which only depend on the gauge couplings which are, of course, flavour independent.

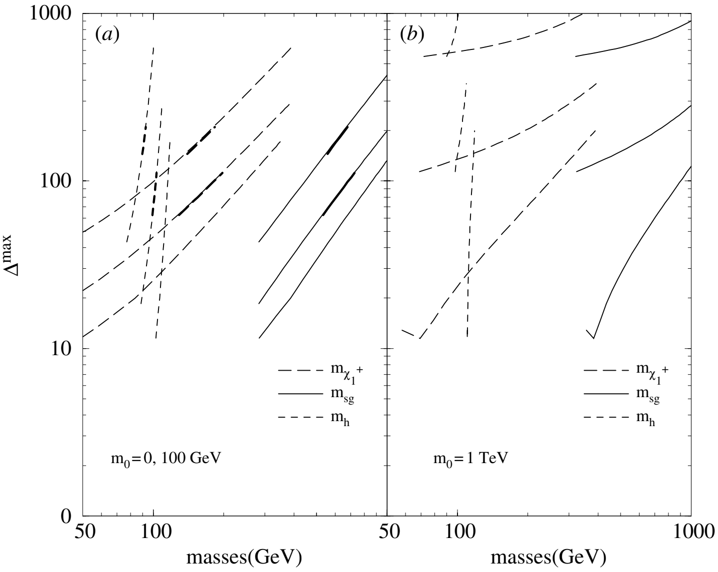

Figure 2. Results for the mSUGRA model. The maximum sensitivity parameter Δ^{max} is plotted as a function of the lightest CP-even Higgs mass (short dashes), gluino mass (solid line) and lightest chargino (long dashes). For each particle type, the three sets of curves correspond to $\tan\beta = 2, 3, 10$, from top left to bottom right, respectively. In (*a*) the shorter, thicker curves correspond to $m_0 = 0$, while the longer curves are those for $m_0 = 100$ GeV. In (*b*) the results correspond to $m_0 = 1000$ GeV.

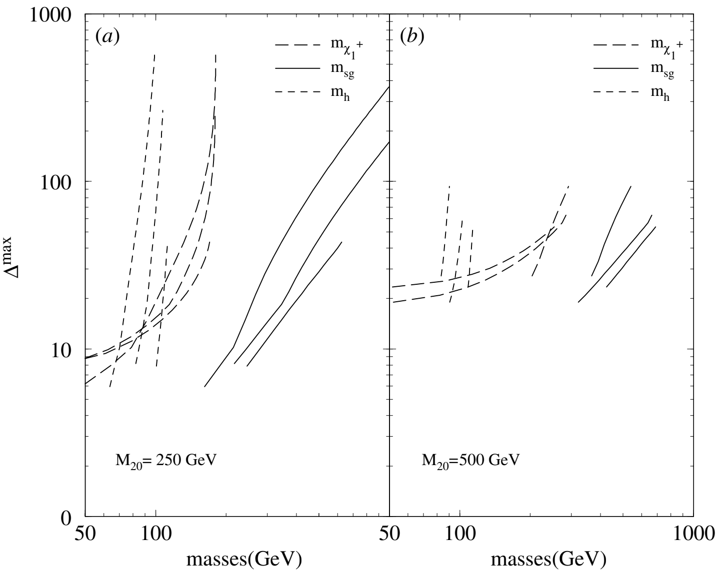

Figure 3. Results for the no-scale with non-universal gaugino masses. The maximum sensitivity parameter Δ^{max} is plotted as a function of the lightest CP-even Higgs mass (short dashes), gluino mass (solid line) and lightest chargino (long dashes). For each particle type, the three sets of curves correspond to $\tan\beta = 2$, 3, 10, from top left to bottom right, respectively. In (*a*) we fix $M_2(0) = 250$ GeV, while in (*b*) $M_2(0) = 500$ GeV.

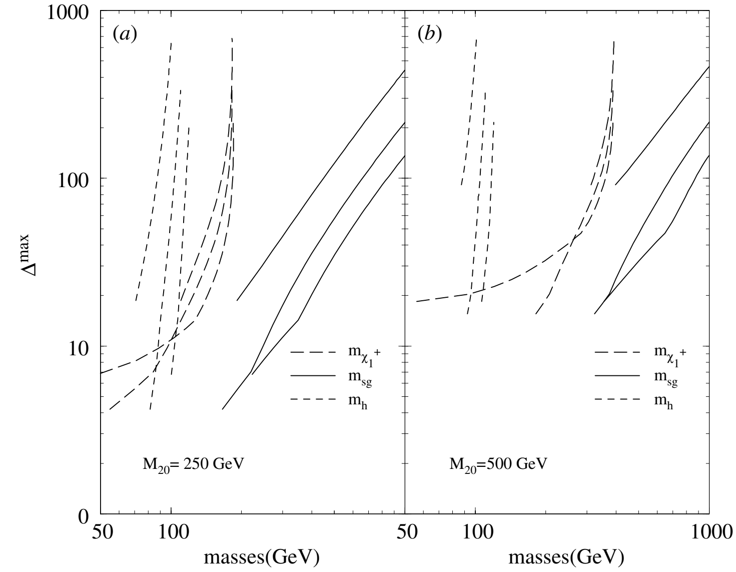

Figure 4. Results for the D-brane model. The maximum sensitivity parameter Δ^{max} is plotted as a function of the lightest CP-even Higgs mass (short dashes), gluino mass (solid curves) and lightest chargino (long dashes). For each particle type, the three sets of curves correspond to $\tan\beta = 2$, 3, 10, from top left to bottom right, respectively. In (*a*) we fix $M_2(0) = 250$ GeV, while in (*b*) $M_2(0) = 500$ GeV.

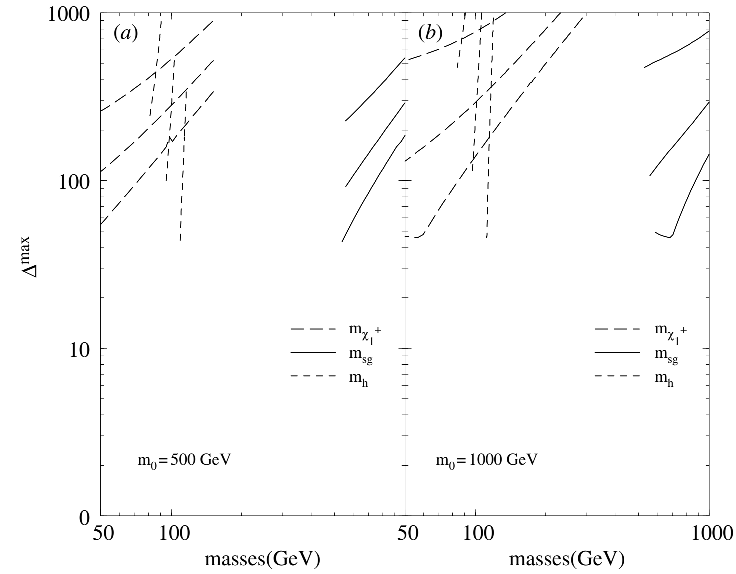

Figure 5. Results for the anomaly-mediated SUSY-breaking model. The maximum sensitivity parameter Δ^{max} is plotted as a function of the lightest CP-even Higgs mass (short dashes), gluino mass (solid curves) and lightest chargino (long dashes). For each particle type, the three sets of curves correspond to $\tan\beta = 2$, 3, 10, from top left to bottom right, respectively. In (*a*) we fix $m_0 = 500$ GeV, while in (*b*) $m_0 = 1000$ GeV.

(iv) Anomaly-mediated SUSY-breaking

$$a_{\rm AMSB} \in \{m_{3/2}, m_0^2, B(0), \mu(0)\}. \qquad (11)$$

Our main results are shown in figures 2–5, corresponding to SUGRA models (i)–(iv) above. In all models, fine-tuning is reduced as $\tan\beta$ is increased, with $\tan\beta = 10$ preferred over $\tan\beta = 2, 3$. Nevertheless, the present LEP2 limit on the Higgs and chargino mass of about 100 GeV and the gluino mass limit of about 250 GeV implies that $\Delta^{\rm max}$ is of order ten or higher. The fine-tuning increases most sharply with the Higgs mass. The Higgs fine-tuning curves are fairly model independent, and as the Higgs mass limit rises above 100 GeV come to quickly dominate the fine-tuning. We conclude that the prospects for the discovery of the Higgs boson at LEP2 are good. For each model there is a correlation between the Higgs, chargino and gluino mass, for a given value of fine-tuning. For example, if the Higgs is discovered at a particular mass value, then the corresponding chargino and gluino mass for each $\tan\beta$ can be read off from figures 2–5.

The new general features of the results may then be summarized as follows:

- The gluino mass curves are less model dependent than the chargino curves, and this implies that in all models if the fine-tuning is not too large then the prospects for the discovery of the gluino at the Tevatron are good.
- The fine-tuning due to the chargino mass is model dependent. For example, in the no-scale model with non-universal gaugino masses and the D-brane scenario the charginos may be relatively heavy compared with mSUGRA.
- Some models have less fine-tuning than others. We may order the models on the basis of fine-tuning from the lowest fine-tuning to the highest fine-tuning: D-brane scenario $<$ generalized no-scale SUGRA $<$ mSUGRA $<$ AMSB.
- The D-brane model is less fine-tuned partly because the gaugino masses are non-universal, and partly because there are large regions where $\Delta_{m_{3/2}}$, $\Delta_{\mu(0)}$, and Δ_θ are all close to zero. However, in these regions the fine-tuning is dominated by Δ_Θ, and this leads to an inescapable fine-tuning constraint on the Higgs and gluino mass.

References

[1] Bastero-Gil M, Kane G L and King S F 1999 *Preprint* hep-ph/9910506

4. Gluino–gluino bound states

V Kartvelishvili and R McNulty

Abstract. The properties of gluinonium are briefly reviewed. We then discuss possibilities for detection at run II of the Tevatron via peaks in the di-jet invariant mass spectrum.

If the decay of a gluino into a quark–squark pair is forbidden kinematically and R-parity is conserved, the gluino can only decay into a quark–antiquark pair and a neutralino, via a virtual squark, with a far longer lifetime. In this case the usual strategies for gluino searches using high P_T jets and missing transverse energies are far less efficient—the jets are more numerous and hence softer, while the missing energy is smaller. Consequently, the reach for gluino searches is significantly reduced and it is quite difficult to obtain a model-independent limit.

In this case, however, there is a possibility of observing the gluino indirectly, by detecting a gluino–gluino bound state (see [1, 2] and references therein). This has the advantage that the conclusions which can be drawn from a search for such states hold in a very wide class of SUSY models. In addition, the detection of such a state would lead to a relatively precise determination of the gluino mass, which could not be obtained easily by observing the decay products of the gluino itself, as some of these escape undetected.

Gluino–gluino bound states (sometimes called gluinonium) can be detected as narrow peaks in the di-jet invariant mass distributions. The main problem is the high background from QCD high P_T jets, and thus it is vital to have di-jet invariant mass resolution as good as possible.

4.1. Properties of gluinonium

As strongly interacting fermions, gluinos have a lot in common with heavy quarks. But there are important differences:

- a gluino has no electroweak coupling, so its lifetime is defined by its strong decays. For our case of interest, $m_{\tilde{g}} < m_{\tilde{q}} + m_q$, this means that the gluino lives long enough to form a bound state;
- a gluino is a colour octet; the potential between two gluinos is attractive not only if they are in a colour-singlet state, but also if they are in colour-octet states, both symmetric and antisymmetric;
- a gluino is a Majorana fermion (i.e. is its own antiparticle), and some gluinonium states are forbidden due to the Pauli principle.

The resulting spectra of low-lying gluinonium states [3] are shown in table 1. The allowed colour-singlet state 1 and symmetric octet 8_S states have the same J^P values as the charmonium states with $C = +1$, while the allowed antisymmetric colour-octet 8_A states have the same J^P values as the charmonium states with $C = -1$. In particular, the lowest-lying colour-singlet and symmetric colour-octet states are the pseudoscalars $\eta^0_{\tilde{g}}$ and $\eta^8_{\tilde{g}}$ with $J^P = 0^-$, while the lowest-lying antisymmetric colour-octet state is vector gluinonium $\psi^8_{\tilde{g}}$ with $J^P = 1^-$.

All three $L = 0$ states decay via gluino–gluino annihilation. The pseudoscalars $\eta^{0,8}_{\tilde{g}}$ decay mainly to two gluons [3] with decay widths $\sim 10^{-3}\ M$, while vector gluinonium $\psi^8_{\tilde{g}}$ decays predominantly into $q\bar{q}$ pairs [4] with a decay width of about $10^{-4}\ M$. Although much larger

Table 1. Spin parities J^P for the allowed low-lying states of gluinonium with $L = 0$. The three columns correspond to the colour-singlet state 1 and the symmetric and antisymmetric colour-octet states 8_S and 8_A, respectively.

	1	8_S	8_A
$^1S_0$	$0^-(\eta^0_{\tilde{g}})$	$0^-(\eta^8_{\tilde{g}})$	
$^3S_1$			$1^-(\psi^8_{\tilde{g}})$

than the free gluino decay width, these widths are still very small compared with the gluinonium mass $M \approx 2m_{\tilde{g}}$. The size of all three states is of order $a^B \equiv 4(\alpha_s M)^{-1}$, which is much smaller than the confinement length, thus justifying the relative stability of the colour-octet states (see [1, 4]).

So, the vector gluinonium $\psi^8_{\tilde{g}}$ is a heavy compact object which behaves rather like a heavy gluon, except that its coupling to quarks is much stronger than its coupling to gluons. Hence it is most readily produced via $q\bar{q}$ annihilation and the Tevatron is a promising place to look, being a source of both valence quarks and valence antiquarks. In contrast, the pseudoscalar states $\eta^0_{\tilde{g}}$ and $\eta^8_{\tilde{g}}$ couple predominantly to gluons, and can be produced equally well in both pp and $\bar{p}p$ collisions via the gluon–gluon fusion mechanism. Their production cross section increases more rapidly with energy than that for vector gluinonium, and there is more chance of detecting them at the LHC.

4.2. *Vector gluinonium at the Tevatron*

The vector gluinonium is produced and decays in $p\bar{p}$ collisions via the subprocess

$$q + \bar{q} \to \psi^8_{\tilde{g}} \to q + \bar{q}, Q + \bar{Q} \tag{12}$$

where we use the symbols q = u, d, s and Q = c, b, t to distinguish light and heavy quarks†.

The nature of the background depends on $M/\sqrt{s}$. At Tevatron energies, the range of interest lies mainly in large values $M/\sqrt{s} > 0.2$, where the luminosity of colliding $q\bar{q}$ pairs prevails over that of gluon–gluon pairs. In this region, the main sources of di-jet background are the subprocesses

$$q + \bar{q} \xrightarrow{\text{QCD}} g + g, q + \bar{q}, Q + \bar{Q} \tag{13}$$

where the first two have the angular dependence $\propto (1 - \cos^2\theta^*)^{-2}$, peaking sharply at $\cos\theta^* = \pm 1$, where θ^* is defined in the c.m. frame of the two jets. In contrast, the signal from the subprocess (12) has a much weaker dependence, $\sim 1 + \cos^2\theta^*$. Hence, a cut $|\cos\theta^*| < z$ should improve the signal-to-background ratio.

The usefulness of heavy quark tagging is clearly brought out by considering the production ratios for the various final states in both the signal (12) and background (13). The relative contribution of the three background subprocesses in (13) at small $|\cos\theta^*|$ is given by [4]

$$gg : q\bar{q} : Q\bar{Q} = 14 : 65 : 6, \tag{14}$$

while for the signal (12) one has

$$gg : q\bar{q} : Q\bar{Q} = 0 : 3 : 2. \tag{15}$$

Hence by tagging the heavy quark jets one reduces the background by a factor of $\frac{85}{6} \approx 14$, while retaining 40% of the signal.

† Obviously, t-quarks contribute only if the gluino is heavy enough, and even then for the range of gluino masses accessible at the Tevatron this contribution is strongly suppressed by the available phase space.

At smaller gluinonium masses $M \approx 2m_{\tilde{g}} < 200$ GeV, initial gluons contribute much more significantly to the background, even with heavy quark jet tagging, through the subprocess

$$g + g \xrightarrow{\text{QCD}} Q + \bar{Q}. \tag{16}$$

This makes the signal-to-background ratio hopelessly small for any realistic two-jet invariant mass resolution. However, this region of gluino masses is already covered by other methods.

4.3. Simulation

So, most of the two-jet QCD background at large invariant masses arises from light quark and gluon jets, and the signal-to-background ratio can be significantly enhanced by triggering on heavy quark jets [4]. To check that this makes the detection of vector gluinonium a viable possibility at the upgraded Tevatron, we have simulated both the gluinonium signal and the two-jet QCD background using PYTHIA 5.7. The vector gluinonium production and decay was simulated by exploiting the fact that $\psi^8_{\tilde{g}}$ behaves much like a heavy Z′ with axial current and lepton couplings set to zero and a known mass-dependent vector current coupling to quarks, chosen to comply with the corresponding decay width after taking into account appropriate colour and flavour counting. This effective coupling included the non-Coulomb corrections and an enhancement due to the fact that numerous radial excitations of the $\psi^8_{\tilde{g}}$, which could not be separated from it for any reasonable mass resolution, will also contribute. These yield an overall factor of between 1.8 and 1.6 depending on M, and the resulting effective vector coupling a_V falls exponentially from $a_V = 0.225$ at $M = 2m_{\tilde{g}} = 225$ GeV to $a_V = 0.172$ at $M = 2m_{\tilde{g}} = 450$ GeV. This signal sits on a much larger background, which has been simulated on the assumption that it arises entirely from the leading-order QCD subprocesses for heavy quark pair production (13) and (16). A constant K factor $K = 2.0$ has been used for both signal and background.

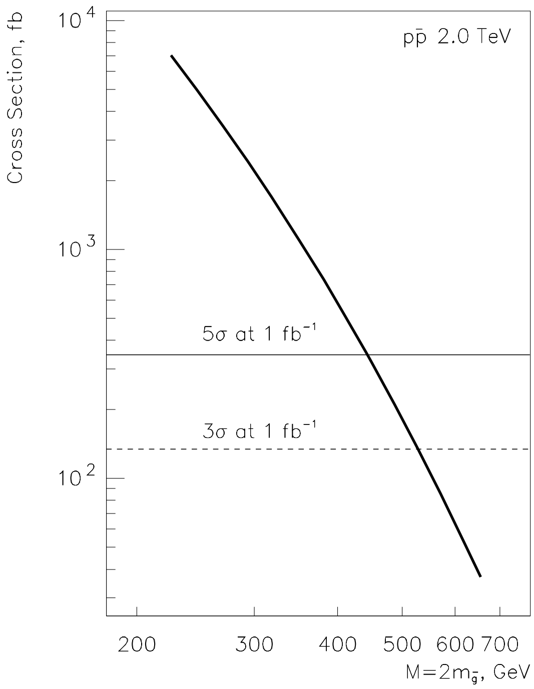

Figure 6. The calculated production cross section of vector gluinonium in $p\bar{p}$ collisions at 2.0 TeV. The solid and broken horizontal lines indicate the cross-sections corresponding to a statistical significance at the peak of five and three standard deviations respectively, for a luminosity of 1 fb^{-1}. (See the text for the cuts and resolutions used.)

The cross section for vector gluinonium production at the upgraded Tevatron with its energy increased to 2 TeV is shown in figure 6. Only decays into heavy quark–antiquark pairs were taken into account, and the tagging efficiency for at least one c- or b-quark jet was assumed to be 50%. The cut on the jet angle θ^* in the two-jet c.m frame was $|\cos\theta^*| < \frac{2}{3}$, and the cut on jet rapidity was $|y| < 2.0$. The signal-to-background ratio was found to be around 7–10% at the peak for the assumed two-jet invariant mass resolutions of 25 GeV, 30 GeV and 38 GeV at $M = 225$ GeV, 320 GeV and 450 GeV respectively. One can hope to see the gluinonium signal from gluinos with masses up to 220 GeV as a five-standard-deviation peak, and the signal from gluinos with masses up to 260 GeV as a three-standard-deviation peak. Note that the statistical significance of the peak is essentially inversely proportional to the two-jet invariant mass resolution, so the reach can be significantly extended if some way is found to improve the latter.

4.4. Conclusion

We conclude that gluinonium states can be detected as narrow peaks in the di-jet invariant mass spectra, effectively complementing more traditional gluino searches, in the case when the gluino is lighter than the squarks.

In $p\bar{p}$ collisions one expects copious production of vector gluinonium, which decays predominantly to $q\bar{q}$ pairs. The high efficiency of the heavy quark jet tagging together with the boost of the Tevatron energy and luminosity should allow one to reach gluino masses of 220–260 GeV at $\sqrt{s} = 2.0$ TeV and 1000 pb^{-1}, with realistic efficiencies, resolutions and experimental cuts taken into account. It is crucial, however, to improve tagging efficiency for both c- and b-quark jets, as well as the two-jet invariant mass resolution for these jets.

References

[1] Haber H R and Kane G L 1984 *Phys. Rep.* **117** 75
[2] Chikovani E, Kartvelishvili V, Shanidze R and Shaw G 1996 *Phys. Rev.* D **53** 6653
[3] Keung W Y and Khare A 1984 *Phys. Rev.* D **29** 2657
Kühn J H and Ono S 1984 *Phys. Lett.* B **142** 436
Goldman T and Haber H E 1985 *Physica* D **15** 181
[4] Chikovani E G, Kartvelishvili V G and Tkabladze A V 1989 *Z. Phys.* C **43** 509
Chikovani E G, Kartvelishvili V G and Tkabladze A V 1990 *Sov. J. Nucl. Phys.* **51** 546

5. Experimental signatures from theories with extra dimensions

J Grosse-Knetter, J Holt and S Lola

Abstract. We discuss possible experimental signatures and distinctions between two models with extra dimensions. In the first model a number n of large extra dimensions is postulated, while the second involves the addition of only one extra dimension, but with a metric which is non-factorizable into 4 + 1 separate dimensions (the Randall–Sundrum model).

An important issue in extending the SM of particle physics, is the hierarchy problem, arising from the existence of two vastly different fundamental scales (M_W and M_{Pl}). There are ways to evade this problem, such as technicolour and SUSY. A third solution which has recently received considerable attention, is to *identify* the Planck scale with the electroweak scale, by introducing extra dimensions into which gravitons are able to propagate. Here, we discuss some experimental aspects of two classes of such models.

5.1. Models with large extra dimensions

The first set of models considered here is the proposal of [1] where the Planck scale, M_{Pl}, is related to the scale of gravitational interactions, M_D, in a space which includes n extra compact dimensions of radius R. In this case, one finds that $R^n M_D^{n+2} = M_{Pl}^2$ [1], where n is the number of the extra dimensions: for $n = 1$, $R \approx 10^{13}$ m which is obviously excluded. However, already for $n = 2$, $R \approx 1$ mm. No effects of the extra dimensions on SM fields in accelerators have been observed, one therefore assumes that our four-dimensional world lies on a brane while the gravitons (which feel the extra dimensions) can propagate on the bulk. Since momentum in extra dimensions is seen as mass in four dimensions, in computing graviton emission one has to sum over a tower of massive Kaluza–Klein states, with masses $m \approx \frac{2\pi n}{R}$. The coupling to any single mode has the normal gravitational strength ($\approx \frac{1}{\overline{M}_{Pl}}$, where $\overline{M}_{Pl} = M_{Pl}/\sqrt{8\pi}$), while the mass of each mode is very small. However the large multiplicity of modes, given approximately by $\approx (ER)^n$, where E denotes the energy that is available to the graviton, increases the effective coupling $1/M_s$ dramatically.

The Feynman rules for the new vertices [2] are calculated from $\mathcal{L} = -\frac{1}{\overline{M}_{Pl}} g^j_{\mu\nu} T^{\mu\nu}$, where j labels the Kaluza–Klein modes. Some features for the interactions that arise in this class of models, which are important for accelerator searches, are the following: (i) the interactions are flavour independent; (ii) the individual modes are very light and couple very weakly, thus may not be produced on resonance; (iii) the spin-2 nature of the graviton can be determined via angular distributions of the cross sections; (iv) the effective coupling scales as $\frac{1}{\overline{M}^2_{Pl}}(ER)^n \approx \frac{E^n}{M_D^{n+2}}$ and therefore a strong energy dependence (with increase of the cross sections as the energy increases) should appear.

5.2. Limits on models with large extra dimensions

The effects of gravity in models with large extra dimensions, have been searched for using the data from a number of experiments in different channels. No evidence for these effects has been found and lower limits on the parameter M_D, as a function of the number of extra dimensions, n, have been obtained from the different sets of data. Some of these limits, taken

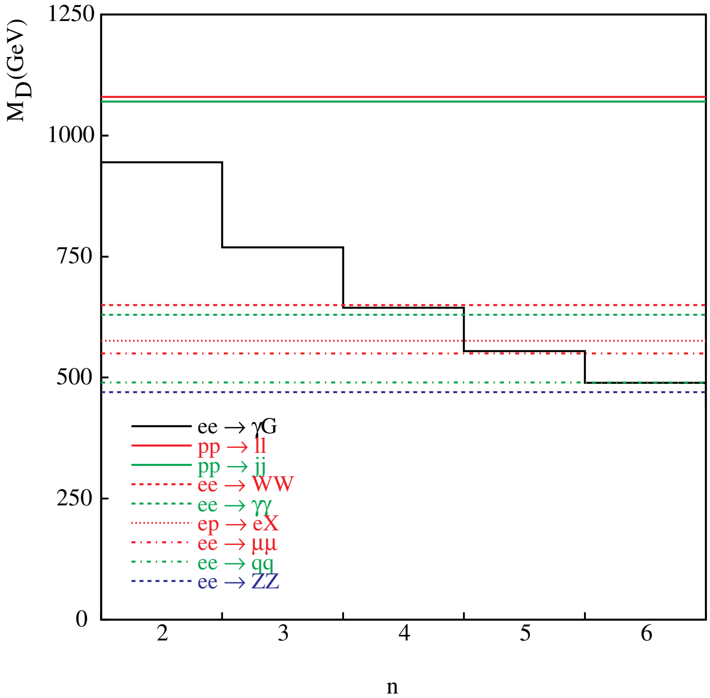

Figure 7. Limits on the scale M_D as a function of the number of extra dimensions n from different channels. References are given in the text.

from [3] together with the results presented below from HERA DIS, are shown in figure 7. The limits coming from $e^+e^- \to \gamma$ graviton at LEP II show a strong dependence on the number of extra dimensions. The cross section for this process depends on the phase space available to the emitted gravitons which depends on n. The other limits are derived from processes which involve virtual exchange of gravitons. The effective string scale M_s has been taken to be equal to M_D. The graviton exchange can interfere constructively or destructively with the SM processes, set by a parameter $\lambda = \pm 1$; the above limits are for $\lambda = +1$

The best limits under these assumptions come from the TEVATRON from di-lepton production using a combination of CDF and D0 data. Limits from CDF alone on di-jet production are very competitive, suggesting that improved sensitivity could be obtained by including D0 di-jet data. Combining all the channels studied by L3 at LEP II, gives a lower limit on M_s of 860 GeV [3] from approximately 50 pb^{-1} of data. The four LEP collaborations now have a total of more than 1.6 fb^{-1} worth of data collected at energies above ∼183 GeV. Combining all results sensitive to virtual graviton exchange, from all four experiments, could give results which would compete with those from the TEVATRON.

5.3. Fits to HERA DIS data

One of the processes with sensitivity to effects predicted from Kaluza–Klein models with large extra dimensions is the NC deep-inelastic scattering (DIS) of positrons off protons. Effects are expected through the exchange of gravitons coupling to both e^+q and e^+g in addition to the SM exchange of photons and Z^0 bosons [6]. These additional contributions (expected at large $Q^2 \approx M_s$) lead to an enhancement in the cross section $d\sigma/dQ^2$, where Q^2 is the squared

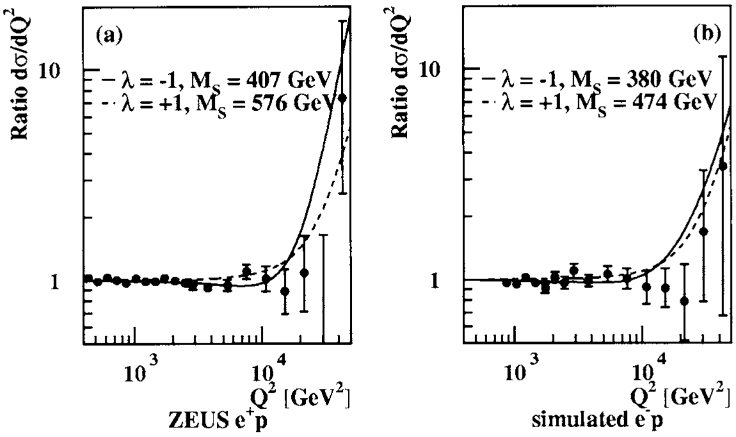

Figure 8. Fits with a model including graviton exchange to HERA NC DIS the cross section $d\sigma/dQ^2$: (*a*) fit to ZEUS e^+p data; (*b*) fit to simulated data corresponding to e^-p data recently taken at HERA.

four-momentum transferred between positron and proton.

Fitting the cross section expected from the combination of the SM and graviton exchange to recent e^+p NC DIS data from ZEUS [7] (similar results are expected from corresponding H1 data [8]) using CTEQ4 PDFs yields 95% CL limits of $M_s > 407$ GeV ($\lambda = -1$) and $M_s > 576$ GeV ($\lambda = +1$) in agreement with expectations based on preliminary data [6]. The results are illustrated in figure 8(*a*) as the ratio of fitted cross section $d\sigma/dQ^2$ to that expected from the SM.

It was further investigated whether the recent HERA e^-p NC DIS data [9] can provide additional information on the mass-scale of extra dimensions. For this purpose e^-p NC DIS data were simulated based on the uncertainty expected from the luminosity of the existing data sample. Fits similar to above were performed as shown in figure 8(*b*) yielding $M_s > 380$ GeV ($\lambda = -1$) and $M_s > 474$ GeV ($\lambda = +1$). Thus, no stricter limits than already obtained from the e^+p data should be expected.

The predicted cross sections for processes at the TEVATRON and HERA are sensitive to uncertainties in the parton distribution functions (PDFs) of the proton. We first estimate the uncertainties in M_s arising from PDF uncertainties in fits to HERA DIS data. For this purpose results are used from a NLO QCD fit [7] to measurements of proton structure functions and quark asymmetries from collider and fixed target experiments. The fit propagates statistical and correlated systematic errors from each experiment to corresponding errors in the PDFs which are used to determine uncertainties in the cross section $d\sigma/dQ^2$, including contributions from graviton exchange. The result is shown as the ratio of $d\sigma/dQ^2$ (SM + graviton) for $M_s = 500$ GeV and $\lambda = -1$ to $d\sigma/dQ^2$ (SM) in figure 9 (left). The band shows the uncertainty in the ratio $d\sigma/dQ^2$ (SM + graviton)/(SM) arising from PDF uncertainties. The latter was compared with the variation in the ratio as M_s changes, for nominal PDFs. These are shown by the dashed and dotted curves, where incremental changes in M_s of 5 GeV are made. This procedure shows that only small errors in M_s, of approximately 15 GeV, arising from PDF uncertainties should be expected.

Similar effects from PDF uncertainties are expected for fits to TEVATRON data. To check the effect of PDF uncertainties on this limit the Drell–Yan cross section $d\sigma/dM$ (M being the

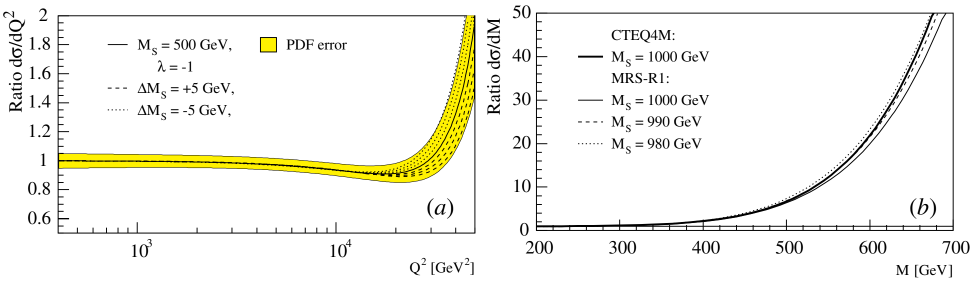

Figure 9. Effect of PDF uncertainties on limits in M_s obtained from fits to the NC DIS cross section $d\sigma/dQ^2$ (left) and to the Drell–Yan cross section $d\sigma/dM$ (right).

hard scale, i.e. the e^+e^- mass) is determined in leading-order QCD with two different PDF sets† including contributions from graviton exchange, in figure 9 (right). This analysis indicates that uncertainties in the limits on M_s resulting from PDF uncertainties should be expected to be of the order of 10–20 GeV.

5.4. Randall–Sundrum in $e^+e^- \to \mu^+\mu^-$ at LEP II

So far, we have been referring to models with more than one extra dimension and with a factorizable metric. One can instead envisage a case where a large mass hierarchy may be generated by an exponential 'warped' factor of a small compactification radius, r_c, in the case of a five-dimensional non-factorizable geometry [4]. It turns out that a field with a fundamental mass parameter m_0 on the visible world appears to have a physical mass $m = e^{-kr_c\pi}m_0$, where k is a scale of the order of the Planck scale, relating the five-dimensional Planck scale M to the cosmological constant. The interaction Lagrangian in the four-dimensional effective theory indicates that, while the zero mode couples with the usual four-dimensional strength, the massive KK states are relatively unsuppressed. Thus, unlike the previous case of more than one factorizable extra dimension, now (i) the individual modes are heavier ($\mathcal{O}$(TeV)); (ii) the individual modes couple with weak interaction strength thus may be produced on resonance; (iii) as one increases the centre-of-mass energy, one may hope to probe a multi-resonance effect.

For instance, for the first mode, the mass, m_1, and the width, Γ_1, of the resonance are given by $m_1 = \Lambda_\pi x_1(k/\overline{M}_{\rm Pl})$ and $\Gamma_1 = \rho m_1 x_1^2(k/\overline{M}_{\rm Pl})^2$ where x_1 is the first non-zero root of the J_1 Bessel function and ρ is a constant which depends on the number of decay channels. Moreover, by making the substitution $\frac{\lambda}{M_s^4} \to \frac{i^2}{8\Lambda_\pi^2}\sum_{n=1}^{\infty}\frac{1}{s-m_n^2-is\Gamma_n/m_n}$ in the formulae obtained for n factorizable extra dimensions, one can proceed to calculate any process. Clearly, as $\frac{k}{M_{\rm Pl}}$ grows, the resonant peaks are substituted by a contact–interaction behaviour.

The possibility of finding a Randall–Sundrum resonance with a mass as low as 100–200 GeV in $e^+e^- \to \mu^+\mu^-$ at LEP II has been investigated. It would be possible to hunt for such a resonance by examining the distribution of the number of muon events observed as a function of the invariant mass, $\sqrt{s'}$, of the pair of muons, taking advantage of initial-state radiation which provides access to invariant masses below the centre-of-mass energy of the LEP collision energy, $\sqrt{s}$.

† The PDF uncertainties from the QCD fit described above were only available for hard scales corresponding to $M < 300$ GeV, so below the range sensitive to graviton exchange, and could thus not be used here.

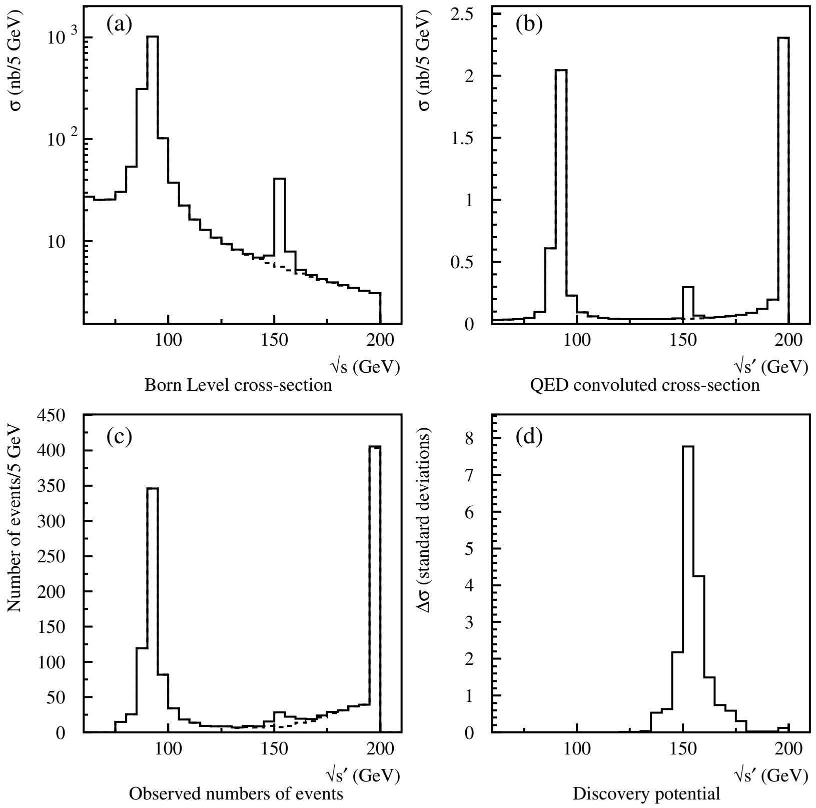

Figure 10. Predictions for the Randall–Sundrum model with $\Lambda_\pi = 800$ GeV and $k/\overline{M}_{\rm Pl} = 0.05$. The width of the Randall–Sundrum resonance with mass of ∼150 GeV is 1 GeV. A centre-of-mass energy of 200 GeV and a luminosity of 200 pb^{-1} have been assumed. In figures (*a*)–(*c*) the solid line is the prediction of the Randall–Sundrum model, the dashed curve is the prediction of the SM.

Born-level predictions for the cross section, $\sigma_0(s)$, of the Randall–Sundrum model with $\Lambda_\pi = 800$ GeV and $k/\overline{M}_{\rm Pl} = 0.05$ are shown in figure 10. The mass of the first resonance is approximately 150 GeV. In principle, the parameter ρ which determines the width can be calculated. For the studies presented here ρ was chosen so that the width of the first resonance was 1 GeV. The QED convoluted cross section as a function of $\sqrt{s'}$ is given by $\sigma(s') = R(s')\sigma_0(s = s')$. The radiator function, R, was computed for bins of s' by computing the Born-level cross section and $\sigma(s')$ in the SM. This was then applied to the predictions including the Randall–Sundrum resonance. The QED convoluted cross section for a centre-of-mass energy of 200 GeV is shown in figure 10(*b*). The predicted numbers of events are shown in figure 10(*c*) for a luminosity of 200 pb^{-1}. The $\sqrt{s'}$ distribution has been smeared to take into account the experimental resolution, which was obtained from a simulation of the DELPHI detector.

The difference between the the Randall–Sundrum model and the SM, $\Delta\sigma$, is shown in figure 10(*d*) in terms of the number of statistical standard deviations on the expected numbers of events. Even taking into account the resolution on $\sqrt{s'}$, it is clear that a Randall–Sundrum resonance with the parameters given above would be observable at LEP II given 200 pb^{-1} at $\sqrt{s} = 200$ GeV. In reality, each of the LEP experiments have this much data collected at centre-of-mass energies between 192 and 202 GeV. The spread of energies should not significantly change the ability to observe such a resonance, or place limits in the $(\Lambda_\pi, k/\overline{M}_{\rm Pl})$ plane. A fit could include all centre-of-mass energies and all other final states in e^+e^- collisions sensitive to the presence of a Randall–Sundrum mode.

References

[1] Arkani-Hamed N, Dimopoulos S and Dvali G 1999 *Phys. Rev.* D **59** 086004
[2] Giudice G F, Rattazzi R and Wells J D 1999 *Nucl. Phys.* B **544** 3
[3] Acciarri M *et al* (L3 Collaboration) 1999 *Phys. Lett.* B **464** 135
Mathews P *et al* 1999 *Preprint* hep-ph/9904232
Gupta A K *et al* 1999 *Preprint* hep-ph/9904234
[4] Randall L and Sundrum R 1999 *Phys. Rev. Lett.* **83** 3370
[5] Davoudiasl H, Hewett J L and Rizzo T G 1999 *Preprint* hep-ph/9909255
[6] Mathews P, Raychaudhuri S and Sridhar K 1999 *Phys. Lett.* B **455** 115
[7] Breitweg J *et al* (ZEUS Collaboration) 1999 *Eur. Phys. J.* C **11** 427
[8] Adloff C *et al* (H1 Collaboration) 1999 *Preprint* DESY 99-107 hep-ex/9908059
[9] H1 Collaboration 1999 *HEP99 (Tampere, Finland, July 1999)* Abstract 157b
ZEUS Collaboration 1999 *HEP99 (Tampere, Finland, July 1999)* Abstract 549
[10] Abe F *et al* (CDF Collaboration) 1999 *Phys. Rev.* D **59** 052002
Abbott B *et al* (D0 Collaboration) 1999 *Phys. Rev. Lett.* **82** 4769

6. Some alternative tests of standard SUSY with events containing isolated leptons and missing p_t at LEP2

D Hutchcroft, J Kalinowski, R McNulty, G Wilson and T Wyatt

Abstract. A number of potential new physics processes can give rise to events containing isolated charged leptons and missing p_t at LEP2. Most attention in this field has been focused on the pair production of equal mass particles, which leads to events containing two leptons of roughly equal momenta. In this paper we discuss potential new physics processes with the following experimental signatures: (i) events containing two leptons of unequal momenta; (ii) events containing a single visible lepton and no other activity in the detector.

In the SM, low multiplicity events containing charged leptons and significant missing transverse momentum, p_t^{miss}, arise from the final state $\ell^+\nu\,\ell^-\bar{\nu}$. The most important SM process contributing to this final state is W^+W^- production in which both W decay leptonically: $W^- \to \ell^-\bar{\nu}$ (with $\ell = e, \mu, \tau$), thus producing events containing an 'acoplanar'† pair of observed leptons. The SM subprocess leading to the final state $W^-e^+\nu$ tends to produce events containing a single observed lepton, since the e^+ has a high probability to be scattered at a small angle to the beam direction and thus escape detection.

Events containing charged leptons and p_t^{miss} are also an experimental signature for the production of new particles that decay to a charged lepton accompanied by one or more invisible particles. For example, acoplanar di-lepton events are a signal for the pair production of new particles such as:

Charged scalar leptons (sleptons). $\tilde{\ell}^\pm \to \ell^\pm\tilde{\chi}_1^0$, where $\tilde{\ell}^\pm$ may be a selectron ($\tilde{e}$), smuon ($\tilde{\mu}$) or stau ($\tilde{\tau}$), $\ell^\pm$ is the corresponding charged lepton and $\tilde{\chi}_1^0$ is the lightest neutralino.

Charged Higgs bosons. $H^\pm \to \tau^\pm\nu_\tau$.

Charginos. $\tilde{\chi}_1^\pm \to \ell^\pm\tilde{\nu}$ ('two-body' decays) or $\tilde{\chi}_1^\pm \to \ell^\pm\nu\tilde{\chi}_1^0$ ('three-body' decays).

A typical candidate event is shown in figure 11.

The LEP detectors provide hermetic detection for showering and minimum ionizing particles, typically down to an angle of around 0.04 rad with respect to the beam direction. This means that the potential background from SM processes such as $e^+e^-\tilde{\ell}^+\tilde{\ell}^-$, which have four charged leptons in the final state (of which only two are observed in the detector), can be reduced to a low level. Such potential backgrounds do, however, mean that the scaled missing transverse momentum of selected events, p_t^{miss}/E_{beam}, has to be required to exceed around 0.04.

A general search for the anomalous production of events of this type can be made by comparing the number and general properties of the selected data with the expectations from the SM. However, because of the very large SM cross section of around 2 pb, such a search is sensitive only to fairly large deviations from the SM expectations. When searching for a particular new particle the sensitivity can be increased by considering an event as a potential candidate only if the properties of the observed event are consistent with expectations for the particular new physics signal under consideration.

† The acoplanarity angle is defined as 180° minus the angle between the two lepton candidates in the plane transverse to the beam direction.

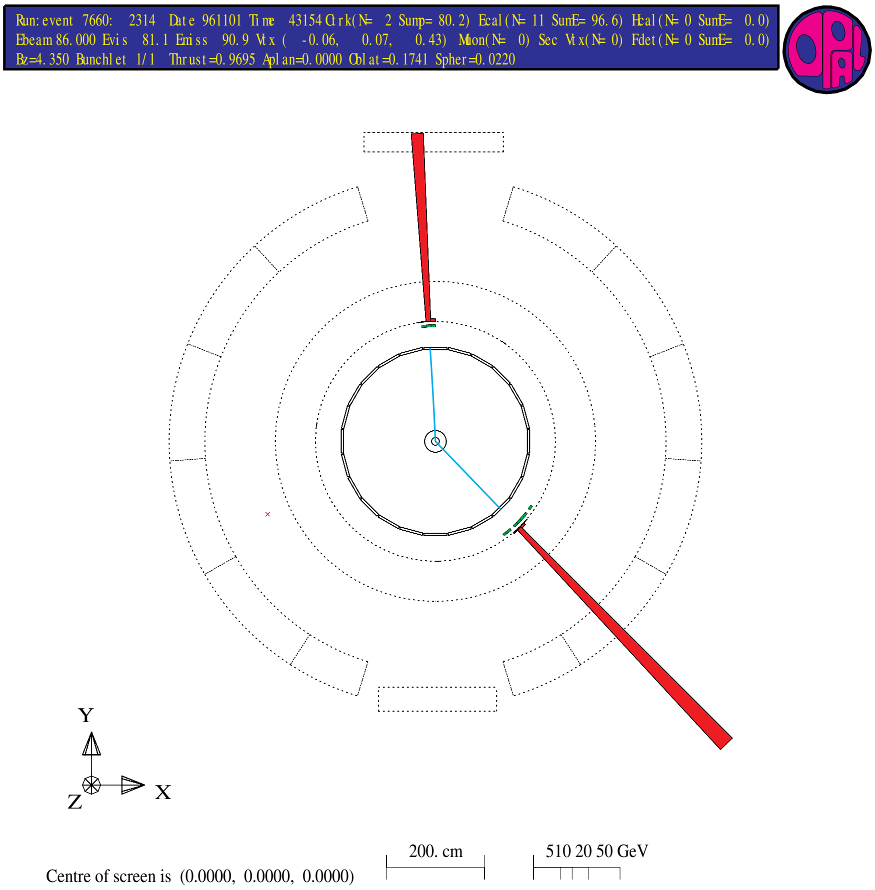

Figure 11. An acoplanar di-lepton candidate selected by OPAL at 172 GeV.

An important property of the selected events that allows new physics sources to be distinguished from the SM $\ell^+\nu\,\ell^-\bar{\nu}$ final states is the momentum of the observed leptons. The SM $\ell^+\nu\,\ell^-\bar{\nu}$ from W^+W^- are characterized by the production of two leptons, both with $p/E_{\rm beam}$ around 0.5. In the SM $e^+e^-\tilde{\ell}^+\tilde{\ell}^-$ events both observed leptons tend to have low momentum. In the new physics signal events the momentum distribution of the expected leptons varies strongly as a function of the mass difference, Δm, between the parent particle (e.g. selectron) and the invisible daughter particle (e.g. lightest neutralino), and, to a lesser extent, m, the mass of the parent particle. When performing a search at a particular point in m and Δm, the SM background can be minimized by considering an event as a potential candidate only if the momenta of the observed leptons are consistent with expectations.

The results of the lepton identification and angular distributions may also help to reduce the SM background in some searches. In SM $\ell^+\nu\,\ell^-\bar{\nu}$ events from W^+W^-, equal numbers of $e^\pm$, $\mu^\pm$ and $\tau^\pm$ are produced and there is no correlation between the flavours of the two charged leptons in the event. Some new physics sources of acoplanar lepton pair events, such as slepton pair production, would produce events in which the two leptons have the same flavour. The charge-signed angular distribution of the leptons in the SM events shows a strong peak in the forward direction due to the dominance of the neutrino exchange amplitude and the

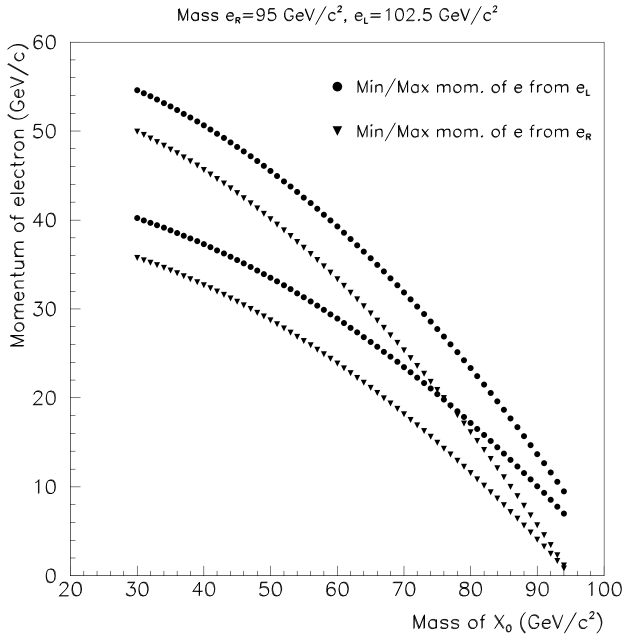

Figure 12. In $\tilde{e}^+_L\tilde{e}^-_R$ production: the kinematically allowed ranges of the momenta of the two observed electrons as a function of $m_{\tilde{\chi}^0_1}$, for the specific choice of $m_{\tilde{e}_R} = 95$ GeV, $m_{\tilde{e}_L} = 102.5$ GeV and $\sqrt{s} = 200$ GeV.

V–A nature of W decay. This is in contrast to the expectation, for example, in smuon, stau and charged Higgs production, in which the angular distribution is forward–backward symmetric and peaked towards $\cos\theta = 0$, due to the scalar nature of these particles.

There is a risk in this approach that the increased sensitivity in the particular individual search channels considered may be obtained at the cost of a lack of generality of the overall search. In order to avoid the danger that a new physics baby might be thrown out with the SM bathwater, it is important to ensure that the widest possible range of experimental signatures from potential new physics sources is searched for.

Searches for new physics in the acoplanar di-lepton channel including the data up to $\sqrt{s} = 189$ GeV have been published by OPAL [1] and ALEPH [2]. Similar searches including the data up to $\sqrt{s} = 183$ GeV have been published by L3 [3] and DELPHI [4]. These analyses tend to focus primarily on the pair production of equal mass particles such as charged scalar leptons ($\tilde{\ell}^+_L\tilde{\ell}^-_L$, $\tilde{\ell}^+_R\tilde{\ell}^-_R$), or leptonically decaying charged Higgs bosons and charginos. In this case, the two observed leptons are expected to have the same momentum spectrum, so that one searches for events containing two high (low) momentum leptons in the case of high (low) Δm.

A possible source of acoplanar lepton pair events with unequal momentum leptons is the associated production of left- and right-chiral selectrons ($\tilde{e}^+_L\tilde{e}^-_R$), since these particles, in general, have different masses. For example, figure 12 shows, for two-body decays $\tilde{\ell}^\pm \to \ell^\pm\tilde{\chi}^0_1$, the kinematically allowed ranges of the momenta of the two observed electrons as a function of the lightest neutralino mass, $m_{\tilde{\chi}^0_1}$, for the specific choice of $m_{\tilde{e}_R} = 95$ GeV, $m_{\tilde{e}_L} = 102.5$ GeV and $\sqrt{s} = 200$ GeV. It can be seen that for low $m_{\tilde{\chi}^0_1}$ (and thus high Δm) the momentum distributions of the two electrons overlap substantially, but that as $m_{\tilde{\chi}^0_1}$ increases (and thus Δm becomes small) the momentum distributions become quite separated.

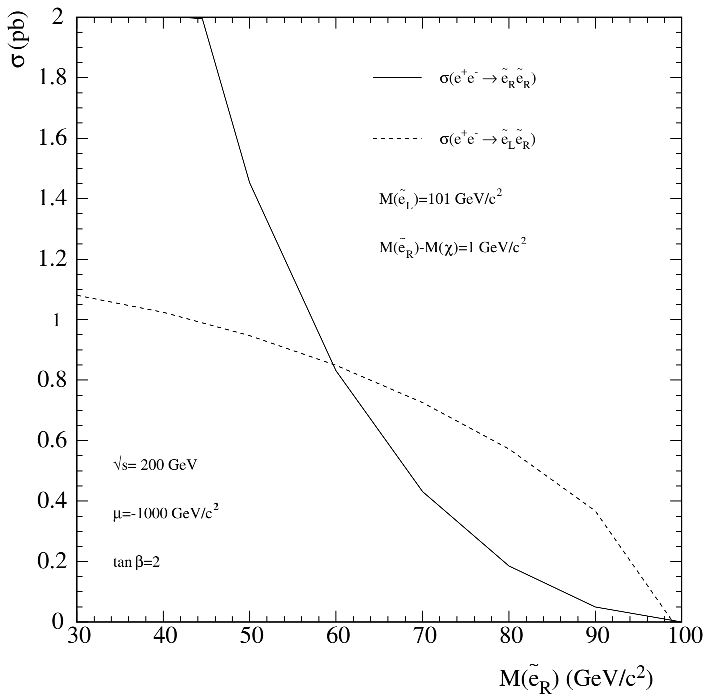

Figure 13. The cross sections for $\tilde{e}^+_L\tilde{e}^-_R$ and $\tilde{e}^+_R\tilde{e}^-_R$ as a function of $m_{\tilde{e}_R}$, for the specific choices $\Delta m = m_{\tilde{e}_R} - m_{\tilde{\chi}^0_1} = 1$ GeV , $m_{\tilde{e}_L} = 101$ GeV and $\sqrt{s} = 200$ GeV.

Another feature of $\tilde{e}^+_L\tilde{e}^-_R$ production that makes it potentially interesting is that, because $\tilde{e}^+_L\tilde{e}^-_R$ results from the t-channel exchange of a $\tilde{\chi}^0_1$, the expected production cross section depends on β/s. This may be contrasted with the β^3/s dependence of the cross section for s-channel production of $\tilde{\ell}^+_L\tilde{\ell}^-_L$ and $\tilde{\ell}^+_R\tilde{\ell}^-_R$. Near to the kinematic limit the cross section for $\tilde{e}^+_L\tilde{e}^-_R$ may be an order of magnitude higher than the pair production cross section for the lightest selectron. This is illustrated in figure 13, in which we compare the cross sections† for $\tilde{e}^+_L\tilde{e}^-_R$ and $\tilde{e}^+_R\tilde{e}^-_R$ as a function of $m_{\tilde{e}_R}$. The cross sections are shown for the specific choices $\Delta m = m_{\tilde{e}_R} - m_{\tilde{\chi}^0_1} = 1$ GeV, $m_{\tilde{e}_L} = 101$ GeV and $\sqrt{s} = 200$ GeV. However, the general features of the plot—that $\sigma_{\tilde{e}^+_L\tilde{e}^-_R}$ is around 100–500 fb and is about an order of magnitude larger than $\sigma_{\tilde{e}^+_R\tilde{e}^-_R}$—are true for a fairly large range of $m_{\tilde{e}_L}$, $m_{\tilde{e}_R}$ and $m_{\tilde{\chi}^0_1}$.

A feasibility study for a search at the example point $m_{\tilde{\chi}^0_1} = 90$ GeV, $m_{\tilde{e}_R} = 95$ GeV, $m_{\tilde{e}_L} = 102.5$ GeV and $\sqrt{s} = 200$ GeV, has been performed using SM and selectron Monte Carlo events‡ processed with a full simulation of the OPAL experiment. From the sample of events that pass a general selection of acoplanar di-lepton events, the lepton identification was required to be consistent with an electron pair and the lepton momenta were required to be in the ranges: $3 < p_1$ (GeV) < 7; $9 < p_2$ (GeV) < 17. (These are significantly broader than the kinematically allowed ranges from figure 12 in order to allow for the effects of detector resolution.) A selection efficiency of around 65% was achieved with a SM expected

† We calculated these cross-sections using the program MSMLIB from [5].

‡ The selectron samples were generated with SUSYGEN [6]. The most important SM samples were generated with KORALZ 4.0 (see Jadach *et al* [6]) and the generator of Vermaseren [6]. All samples were processed with the full simulation program of the OPAL experiment (see Allison *et al* [6]).

background of 8 fb. With an integrated luminosity of 500 pb^{-1} per experiment collected at LEP2, such searches are clearly feasible and should be performed.

How to organize such a search does present some problems, however. In the more standard search for pair production of equal mass particles there are two unknown masses, e.g. $m_{\tilde{\ell}}$ and $m_{\tilde{\chi}_1^0}$. Signal Monte Carlo events have to be generated, event selection cuts or multivariate discriminants have to be optimized, and limits have to be calculated, at each point in a finely spaced grid that covers the whole of the kinematically allowed region of this 2D parameter space. This is time consuming, but achievable. A search for the associated production of unequal mass particles involves three unknown masses, e.g. $m_{\tilde{e}_L}$, $m_{\tilde{e}_R}$ and $m_{\tilde{\chi}_1^0}$. Further work is needed to determine how best to perform the experimental search and present limits in this 3D parameter space.

The associated production of $\tilde{e}_L^+\tilde{e}_R^-$ clearly motivates the search for events containing two electrons of unequal momentum. However, this is no reason to limit the experimental search to electron pair events. In addition to grounds of experimental generality, specific new physics models predict the possibility of observing acoplanar lepton pairs of unequal momentum with arbitrary lepton flavour. For example, [7] describes the scenario of W^+W^- production in which one W decays normally and the other decays via $W^\pm \to \tilde{\chi}_1^0\tilde{\chi}_1^\pm$ followed by $\tilde{\chi}_1^\pm \to \ell^\pm\tilde{\nu}$. If the mass difference between $\tilde{\chi}_1^\pm$ and $\tilde{\nu}$ is less than about 2 GeV the direct searches for $\tilde{\chi}_1^+\tilde{\chi}_1^-$ followed by $\tilde{\chi}_1^\pm \to \ell^\pm\tilde{\nu}$, such as [1], are insensitive because the events contain two very soft leptons with insufficient p_t^{miss} to be selected as acoplanar di-lepton candidates. In contrast, the W^+W^- events considered above have a large p_t^{miss} from the normally decaying W. The soft lepton from the $W^\pm \to \tilde{\chi}_1^0\tilde{\chi}_1^\pm$ decay is visible down to a p_t of 50–100 MeV.

It is interesting to search also for the anomalous production of events containing a single observed lepton. This has been done by the LEP experiments, e.g., in the context of their selection of 'single-W' events ($W^-e^+\nu$ final state) [8]. An example of a potential new physics source of such events is the final state $\tilde{\chi}_1^-e^+\tilde{\nu}$, with the e^+ scattered at a small angle to the beam direction and thus unobserved. An additional interest in this process is provided by the fact that, whereas the pair production of charginos is clearly limited to $m_{\tilde{\chi}_1^\pm} < E_{\mathrm{beam}}$, the final state $\tilde{\chi}_1^-e^+\tilde{\nu}$ is kinematically possible for $m_{\tilde{\chi}_1^\pm} > E_{\mathrm{beam}}$. Unfortunately, the expected cross section is quite small. For the specific example: $m_{\tilde{\chi}_1^\pm} = 100$ GeV, $m_{\tilde{\nu}} = 45$ GeV and $\sqrt{s} = 200$ GeV, the expected cross section is about 20 fb. We calculated this result by using the effective photon approximation and the results on photon–electron scattering in [9]. A feasibility study using Monte Carlo events [6] processed with a full simulation of the OPAL experiment suggests that a selection efficiency of about 60% can be achieved for such events by requiring a single lepton, significant p_t^{miss} and no other activity in the event. However, the predicted SM background is around 200 fb. Although the lepton momentum may give some additional discrimination, it looks difficult to achieve the sensitivity required to observe the expected cross section. Another potential source of events containing a single observed lepton is the final state $\tilde{\chi}_1^0\tilde{e}^+e^-$, although the expected cross section is even smaller than for $\tilde{\chi}_1^-e^+\tilde{\nu}$.

Acknowledgment

JK was partially supported by KBN grant number 2P03B 030 14.

References

[1] Abbiendi G *et al* (OPAL Collaboration) 1999 *Eur. Phys. J.* submitted
(Abbiendi G *et al* (OPAL Collaboration) 1999 *Preprint* CERN-EP/99-122 hep-ex/9909552)

[2] Barate R *et al* (ALEPH Collaboration) 1999 *Phys. Lett.* B **469** 303

(Barate R *et al* (ALEPH Collaboration) 1999 *Preprint* CERN-EP/99-140)
[3] Acciarri M *et al* (L3 Collaboration) 1998 *Eur. Phys. J.* C **4** 207
[4] Abreu P *et al* (DELPHI Collaboration) 1999 *Eur. Phys. J.* C **6** 385
[5] Ganis G Private communication
[6] Katsanevas S and Melachroinos S 1996 *Physics at LEP2* vol 2, ed G Altarelli, T Sjöstrand and F Zwirner (CERN 96-01) p 216
Katsanevas S and Morawitz P 1998 *Comput. Phys. Commun.* **112** 227
Jadach S, Ward B F L and Wąs Z 1994 *Comput. Phys. Commun.* **79** 503
Vermaseren J A M 1983 *Nucl. Phys.* B **229** 347
Allison J *et al* 1992 *Nucl. Instrum. Methods* A **317** 47
[7] Kalinowski J 1997 *Acta Phys. Pol.* B **28** 1437
Kalinowski J and Zerwas P M 1997 *Phys. Lett.* B **400** 112
[8] Acciarri M *et al* (L3 Collaboration) 1998 *Phys. Lett.* B **436** 417
Barate R *et al* (ALEPH Collaboration) 1999 *Phys. Lett.* B **462** 389
[9] Hesselbach S and Fraas H 1997 *Phys. Rev.* D **55** 1343

7. Implications of LEP precision electroweak data for Higgs searches beyond the SM

B C Allanach, J J van der Bij, G G Ross and M Spira

Abstract. We briefly review precision electroweak fits, focusing upon their implications for the SM Higgs mass. We review attempts to extend the analysis beyond the SM in order to obtain information upon Higgs masses in a general scenario.

Figure 14 displays the implications of the combined LEP Electroweak Working Group fit to the minimal SM for the mass of the Higgs boson. From the figure, one can extract

$$m_{h^0} < 230 \text{ GeV at } 95\% \text{ CL} \tag{17}$$

even accounting for the theoretical uncertainty in its determination. The figure shows that the value of m_{h^0} most favoured by the fit is already excluded by the direct searches at LEP, favouring imminent discovery within the context of the SM. It is tempting to infer from the fit that any model beyond the SM must have something that behaves just like a Higgs boson with mass less than 230 GeV, providing the LHC, for example, with complete coverage in its Higgs search. We now provide brief reviews of recent literature which critically examine this inference.

A number of authors [3,4] have used effective Lagrangians to describe low-energy effects of beyond the SM physics. Assuming the SM with Higgs ϕ, one can add the effective Lagrangian pieces [4]

$$-\frac{a}{2!\Lambda^2}\{[D_\mu, D_\nu]\phi\}^\dagger[D^\mu, D^\nu]\phi + \frac{\tilde{b}\kappa^2}{2!\Lambda^2}(\phi^\dagger \overleftrightarrow{D}^\mu \phi)(\phi^\dagger \overleftrightarrow{D}_\mu \phi), \tag{18}$$

where a and $\tilde{b}$ are expected to be of order one. Λ represents the mass scale associated with new physics and κ is a measure of the size of its dimensionless couplings (of order 4π for a strongly

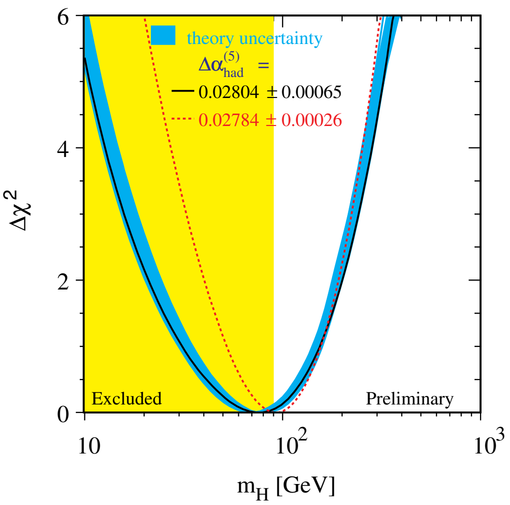

Figure 14. The LEP Electroweak Working Group's fit to Higgs mass [2]. The light shaded area is excluded by the direct Higgs search. The dotted and full curves show two different values for the hadronic part of the extraction of the fine-structure constant $\Delta\alpha^{(5)}_{\rm had}$.

coupled theory). The terms in equation (18) then parametrize the effect of the new physics upon the Higgs. They lead to corrections to the Peskin–Takeuchi S and T parameters [5]

$$\Delta S = \frac{4\pi a v^2}{\Lambda^2}, \qquad \text{and} \qquad \Delta T = \frac{b\kappa v^2}{\alpha\Lambda^2} \tag{19}$$

which are extracted from electroweak fits and strongly constrain physics beyond the SM. Without the operators in equation (18), $\Delta S = \Delta T = 0$ and one retains the prediction in equation (17). When the additional operators are included, the authors of [4] conclude that satisfactory electroweak fits are obtained if

$$m_{\mathrm{H}} < 500\ \mathrm{GeV}, \qquad \Lambda < 10\ \mathrm{TeV}, \tag{20}$$

without unnatural cancellations between the parameters a, b, κ, Λ.

Another approach [3] abandons the Higgs completely and asks the question: can the electroweak data be explained by the SM without a Higgs but with some unspecified (other) new physics? The parameter Λ then defines the scale of the physics responsible for the electroweak symmetry breaking. Gauged chiral Lagrangians provide a model-independent description of the effect of the electroweak symmetry-breaking physics upon low-energy phenomena. The Lagrangian is constructed from the Goldstone bosons w^a coming from the electroweak symmetry breaking. The w^a appear in the group element $\Sigma = \exp(2\mathrm{i}w^a\tau^a/v)$, where τ^a are Pauli matrices, normalized to $\frac{1}{2}$, and $v = 256$ GeV is the scale of the symmetry breaking. The gauge bosons appear through their field strengths, $W_{\mu\nu} = W^a_{\mu\nu}\tau^a$ and $B_{\mu\nu} = B^3_{\mu\nu}\tau^3$, as well as through the covariant derivative, $D_\mu\Sigma = \partial_\mu\Sigma + \mathrm{i}gW^a_\mu\tau^a\Sigma - \mathrm{i}g'\Sigma B^3_\mu\tau^3$. The gauged chiral Lagrangian is built from these objects. It can be organized in a derivative expansion,

$$L = L^{(2)} + L^{(4)} + \cdots, \tag{21}$$

where

$$L^{(2)} = \frac{v^2}{4}\,\mathrm{Tr}\,D_\mu\Sigma D_\mu\Sigma^\dagger + \frac{g'^2 v^2}{16\pi^2} b_1 (\mathrm{Tr}\,T\Sigma^\dagger D_\mu\Sigma)^2 + \frac{gg'}{16\pi^2} a_1\,\mathrm{Tr}\,B_{\mu\nu}\Sigma^\dagger W_{\mu\nu}\Sigma \tag{22}$$

and $T = \Sigma^\dagger\tau^3\Sigma$. a_1, b_1 are the dimensionless couplings associated with the new physics and have been normalized so they would be naturally of order 1 for a strongly interacting sector at $\Lambda \sim 3$ TeV. From equation (22), the authors of [3] obtain

$$\begin{aligned} S &= -\frac{a_1}{\pi} + \frac{1}{6\pi}\log\left(\frac{\Lambda}{M_Z}\right), \\ T &= \frac{b_1}{\pi\cos^2\theta_{\mathrm{W}}} - \frac{3}{8\pi\cos^2\theta_{\mathrm{W}}}\log\left(\frac{\Lambda}{M_Z}\right). \end{aligned} \tag{23}$$

When incorporated into a fit of electroweak precision observables, the above scheme provides acceptable fits without unnatural cancellations between a_1 and b_1 and the second terms in S and T for

$$\Lambda \leqslant 3\ \mathrm{TeV}. \tag{24}$$

Some comments about this last result are in order. The main concern about the result is that the mechanism of electroweak symmetry breaking would be hidden from the LHC. However, if the scale of the new physics were of the order of 3 TeV, the LHC might still see some signals of strongly interacting W, for example longitudinal W pair production [6]. It remains to be seen whether a model can be built which gives a_1, b_1 and Λ of the correct values to fit the electroweak data. For example, the most naive technicolour theories predicted the wrong sign for a_1 compared with the fit and were consequently ruled out [5]. The model then has to simultaneously *not* generate four-fermion effective interactions which are excluded by current data. The above analysis does not include these fermion interactions.

In the SM with Higgs, m_{H} replaces Λ in equation (23). The coefficient in front of the logarithm is the same in both cases. Since we do not know m_{H} (or Λ), S and T are not uniquely predicted. However, the Higgs-mass or Λ-independent combination

$$V \equiv \tfrac{8}{3} T \cos^2 \theta_{\mathrm{W}} + 6S = 0 \tag{25}$$

is a firm prediction of the SM. With the precise measurement of M_{W}, a second Higgs mass-independent prediction can be made based on the U parameter. We think it would be useful, in order to test whether the data are in agreement with the SM *independent of the mechanism of electroweak symmetry breaking*, that two-dimensional plots in U–V space be made, particularly because the fit to the SM is only moderately good.

Acknowledgments

We would like to thank J Forshaw and G Weiglein for helpful discussions.

References

[1] LEP C collaboration meeting *(CERN, Nov 1999)*
[2] LEP electroweak working group see http://www.cern.ch/LEPEWWG/plots/
[3] Bagger J A, Falk A F and Swartz M 1999 *Preprint* hep-ph/9908327
[4] Chivukula R S and Evans N 1999 *Phys. Lett.* B **464** 244
[5] Peskin M E and Takeuchi T 1990 *Phys. Rev. Lett.* **65** 964
[6] ATLAS Collaboration 1999 *Detector and Physics Performance TDR* vol 2 *Technical Report* CERN/LHCC 99-15

8. The stealthy type of Higgs models

J J van der Bij

Abstract. We briefly review the effects of singlet scalars on the Higgs sector.

8.1. Introduction

Understanding of the electroweak symmetry breaking mechanism is one of the main tasks in particle physics. The establishment of the structure of the Higgs sector would be a breakthrough in our knowledge about matter. So it is important to think about alternatives to the SM Higgs sector. Most alternatives give rise to some effects at low energy, that can be measured at LEP and are therefore already constrained. However the simplest possible extension, by scalar singlets, does not give rise to extra radiative corrections at the one-loop level and is therefore indistinguishable from the SM as far as precision measurements at LEP1 are concerned. While leaving the gauge-sector of the SM unchanged singlets can have important effects within the Higgs sector of the model. For example strong interactions can be present. These effects can significantly change the Higgs signal at future colliders. Singlets change the Higgs signal in two ways, mixing and invisible decay, which can appear separately or in combination.

8.2. Mixing

A pure mixing model for singlets was analysed in [1]. This model is the simplest possible extension of the SM, containing only two extra parameters. The Lagrangian of the Higgs sector is given by

$$\mathcal{L} = -\frac{1}{2}(D_\mu\Phi)^\dagger(D_\mu\Phi) - \frac{1}{2}(\partial_\mu X)^2 - \frac{\lambda_1}{8}(\Phi^\dagger\Phi - f_1^2)^2 - \frac{\lambda_2}{8}(2f_2X - \Phi^\dagger\Phi)^2$$

where Φ is the standard Higgs doublet and X a real scalar singlet. After spontaneous symmetry breaking and diagonalization of the mass matrix one finds two Higgs with different masses and each having a reduced coupling g_i to matter: $g_1 = g_{\mathrm{SM}}\cos(\theta)$, $g_2 = g_{\mathrm{SM}}\sin(\theta)$. The branching ratio of decay products is the same as for the SM with the same mass. This model will therefore give rise to two Higgs peaks at the LHC, each with reduced significance. In the mass range where the Higgs can only be studied by rare decays this could marginalize the Higgs signal. The situation is however worse. One can consider not just one X-field, but many [2]. In this case the Higgs signal can be spread out over a large energy range, thereby hiding the Higgs signal at the LHC. However at a linear e^+e^--collider one can use the process $e^+e^- \to ZH$ to study this process.

8.3. Invisible decay

To check the influence of a hidden sector we will study the coupling of a Higgs boson to an $O(N)$ symmetric set of scalars [3]. The effect of the extra scalars is practically the presence of a possibly large invisible decay width of the Higgs particle. When the coupling is large enough the Higgs resonance can become wide even for a light Higgs boson.

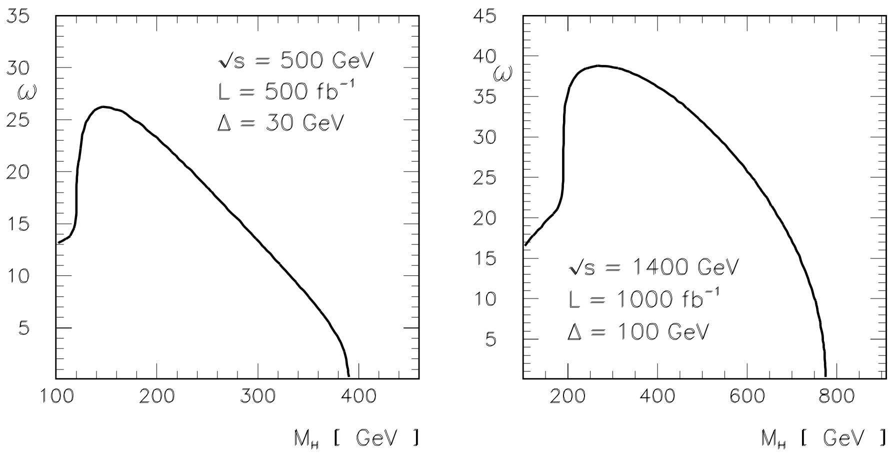

Figure 15. Exclusion limits at a LC at an energy of 500 (1400) GeV and luminosity 500 (1000) fb^{-1}, respectively.

The scalar sector of the model consists of the usual Higgs sector coupled to a real N-component vector $\vec{\varphi}$ of scalar fields, denoted by phions in the following. The Lagrangian density is given by

$$\mathcal{L} = -D_\mu \Phi^+ D_\mu \Phi - \lambda\left(\Phi^+\Phi - \frac{v^2}{2}\right)^2 - \frac{1}{2}\partial_\mu\vec{\varphi}\partial^\mu\vec{\varphi} - \frac{1}{2}m^2\vec{\varphi}^2$$
$$-\frac{\kappa}{(8N)}(\vec{\varphi}^2)^2 - \frac{\omega}{(2\sqrt{N})}\vec{\varphi}^2\Phi^+\Phi$$

where ϕ is the standard Higgs doublet. Couplings to fermions and vector bosons are the same as in the SM. The ordinary Higgs field acquires the VEV $v/\sqrt{2}$. For positive ω the $\vec{\varphi}$-field acquires no VEV. After spontaneous symmetry breaking one is left with the ordinary Higgs boson, coupled to the phions into which it decays. Also the phions receive an induced mass from the spontaneous symmetry breaking which is suppressed by a factor of $1/\sqrt{N}$. If the factor N is taken to be large, the model can be analysed with $1/N$-expansion techniques. By taking this limit the phion mass is suppressed, whereas the decay width of the Higgs boson is not. Because the Higgs width is now depending on the Higgs phion coupling its value is arbitrary. Therefore the main effect of the presence of the phions is to give a possibly large invisible decay rate to the Higgs boson. The invisible decay width is given by

$$\Gamma_\mathrm{H} = \frac{\omega^2 v^2}{32\pi M_\mathrm{H}} = \frac{\omega^2(\sin\theta_\mathrm{W}\cos\theta_\mathrm{W} M_\mathrm{Z})^2)}{32\pi^2\alpha_\mathrm{em} M_\mathrm{H}}.$$

The model is different from Majoron models [4], since the width is not necessarily small. The model is similar to the technicolour-like model of [5].

It is clear that looking for an invisibly decaying wide Higgs resonance is essentially hopeless at the LHC. One should therefore study the signal at a linear e^+e^--collider. A typical exclusion plot is given in figure 1 (taken from [6]).

8.4. The general case

In the general case there will be both mixing and invisible decay. This can be arranged, i.e. by spontaneously breaking the O(N) symmetry in the model above or by allowing X^3, X^4

interactions in the first model. A model of this type was presented in [7]. The general picture consists, therefore, of a Higgs sector that consists of an arbitrary number of mass peaks, with an arbitrary invisible width. The analysis of this general situation is not significantly different from the special cases studied above. The general conclusion is that the LHC might very well be unable to establish a Higgs sector of this type. However, an e^+e^--collider will be able to study such a Higgs sector using the process $e^+e^- \to ZH$ [3, 6, 8]. This can be done in a clean way using the decay of the Z boson to leptons if a high luminosity is provided.

Acknowledgments

This work was supported by the ARC-Program, the DFG-Forschergruppe Quantenfeldtheorie, Computeralgebra und Monte Carlo Simulation and by the NATO-grant CRG 970113.

References

[1] Hill A and van der Bij J J 1987 *Phys. Rev.* D **36** 3463
[2] Krasnikov N V 1998 *Mod. Phys. Lett.* A **13** 893
[3] Binoth T and van der Bij J J 1997 *Z. Phys.* C **75** 17 and references therein
[4] Valle J *et al* 1996 *LEP2 Higgs Report* CERN 96-01 p 350
[5] Chivukula R S and Golden M 1991 *Phys. Lett.* B **267** 233
[6] Binoth T and van der Bij J J 1999 *Linear Collider Workshop (Sitges, 1999)*
[7] Bjorken J D 1992 *Int. J. Mod. Phys.* A **7** 4221
[8] Espinosa J R and Gunion J F 1999 *Phys. Rev. Lett.* **82** 1084

9. Upper limit on m_h in the MSSM and mSUGRA versus prospective reach of LEP

A Dedes, S Heinemeyer, P Teixeira-Dias and G Weiglein

Abstract. The upper limit on the lightest $\mathcal{CP}$-even Higgs boson mass, m_h, is analysed within the MSSM as a function of $\tan\beta$ for fixed m_t and M_{SUSY}. The impact of recent diagrammatic two-loop results on this limit is investigated. We compare the MSSM theoretical upper bound on m_h with the lower bound obtained from experimental searches at LEP. We estimate that with the LEP data taken until the end of 1999, the region $m_h < 108.2$ GeV can be excluded at the 95% CL. This corresponds to an excluded region $0.6 \lesssim \tan\beta \lesssim 1.9$ within the MSSM for $m_t = 174.3$ GeV and $M_{SUSY} \leqslant 1$ TeV. The final exclusion sensitivity after the end of LEP, in the year 2000, is also briefly discussed. Finally, we determine the upper limit on m_h within the mSUGRA scenario up to the two-loop level, consistent with radiative electroweak symmetry breaking (REWSB). We find an upper bound of $m_h \approx 127$ GeV for $m_t = 174.3$ GeV in this scenario, which is slightly below the bound in the unconstrained MSSM.

9.1. Introduction

Within the MSSM the masses of the $\mathcal{CP}$-even neutral Higgs bosons are calculable in terms of the other MSSM parameters. The mass of the lightest Higgs boson, m_h, has been of particular interest, as it is bounded to be smaller than the Z-boson mass at the tree level. The one-loop results [1–4] for m_h have been supplemented in the last years with the leading two-loop corrections, performed in the RG approach [5, 6], in the effective potential approach [7] and most recently in the Feynman-diagrammatic (FD) approach [8, 9]. The two-loop corrections have turned out to be sizeable. They can change the one-loop results by up to 20%.

Experimental searches at LEP now exclude a light MSSM Higgs boson with a mass below $\sim$90 GeV [10–13]. In the low-$\tan\beta$ region, in which the limit is the same as for the SM Higgs boson, a mass limit of even $m_h \gtrsim 106$ GeV has been obtained [10–13]. Combining this experimental bound with the theoretical upper limit on m_h as a function of $\tan\beta$ within the MSSM, it is possible to derive constraints on $\tan\beta$. In this paper we investigate for which MSSM parameters the maximal m_h values are obtained and discuss in this context the impact of the new FD two-loop result. Resulting constraints on $\tan\beta$ are analysed on the basis of the present LEP data and of the prospective final exclusion limit of LEP.

The mSUGRA scenario provides a relatively simple and constrained version of the MSSM. In this paper we explore how the maximum possible values for m_h change compared with the general MSSM, if one restricts oneselves to the mSUGRA framework. As an additional constraint we impose that the condition of REWSB [14] should be fulfilled.

9.2. The upper bound on m_h in the MSSM

The most important radiative corrections to m_h arise from the top and scalar top sector of the MSSM, with the input parameters m_t, M_{SUSY} and X_t. Here we assume the soft SUSY breaking parameters in the diagonal entries of the scalar top mixing matrix to be equal for simplicity, $M_{SUSY} = M_{\tilde{t}_L} = M_{\tilde{t}_R}$. This has been shown to yield upper values for m_h which comprise also the case where $M_{\tilde{t}_L} \neq M_{\tilde{t}_R}$, if M_{SUSY} is identified with the heavier one of $M_{\tilde{t}_L}$, $M_{\tilde{t}_R}$ [9]. For the off-diagonal entry of the mixing matrix we use the convention

$$m_t X_t = m_t(A_t - \mu\cot\beta). \qquad (26)$$

Note that the sign convention used for μ here is the opposite of the one used in [15].

Since the predicted value of $m_{\rm h}$ depends sensitively on the precise numerical value of $m_{\rm t}$, it has become customary to discuss the constraints on $\tan\beta$ within a so-called 'benchmark' scenario (see [16] and references therein), in which $m_{\rm t}$ is kept fixed at the value $m_{\rm t} = 175$ GeV and in which furthermore a large value of $M_{\rm SUSY}$ is chosen, $M_{\rm SUSY} = 1$ TeV , giving rise to large values of $m_{\rm h}(\tan\beta)$. In [17] it has recently been analysed how the values chosen for the other SUSY parameters in the benchmark scenario should be modified in order to obtain the maximal values of $m_{\rm h}(\tan\beta)$ for given $m_{\rm t}$ and $M_{\rm SUSY}$. The corresponding scenario ($m_{\rm h}^{\rm max}$ scenario) is defined as [17, 18]

$$\begin{aligned}
&m_{\rm t} = m_{\rm t}^{\rm exp} (= 174.3 \text{ GeV}), \qquad M_{\rm SUSY} = 1 \text{ TeV}, \qquad \mu = -200 \text{ GeV}, \\
&M_2 = 200 \text{ GeV}, \qquad M_A = 1 \text{ TeV}, \qquad m_{\tilde{\rm g}} = 0.8 M_{\rm SUSY} (\text{FD}) \\
&X_{\rm t} = 2 M_{\rm SUSY} (\text{FD}) \qquad \text{or} \qquad X_{\rm t} = \sqrt{2} M_{\rm SUSY} (\text{RG}),
\end{aligned} \tag{27}$$

where the parameters are chosen such that the chargino masses are beyond the reach of LEP2 and that the lightest $\mathcal{CP}$-even Higgs boson does not dominantly decay invisibly into neutralinos. In equation (27) μ is the Higgs mixing parameter, M_2 denotes the soft SUSY breaking parameter in the gaugino sector, and M_A is the $\mathcal{CP}$-odd Higgs boson mass. The gluino mass, $m_{\tilde{\rm g}}$, can only be specified as a free parameter in the FD result (program FeynHiggs [19]). The effect of varying $m_{\tilde{\rm g}}$ on $m_{\rm h}$ is up to ± 2 GeV [9]. Within the RG result (program subhpole [5]) $m_{\tilde{\rm g}}$ is fixed to $m_{\tilde{\rm g}} = M_{\rm SUSY}$. Compared with the maximal values for $m_{\rm h}$ (obtained for $m_{\tilde{\rm g}} \approx 0.8\, M_{\rm SUSY}$) this leads to a reduction of the Higgs boson mass by up to 0.5 GeV. Different values of $X_{\rm t}$ are specified in equation (27) for the results of the FD and the RG calculation, since within the two approaches the maximal values for $m_{\rm h}$ are obtained for different values of $X_{\rm t}$. This fact is partly due to the different renormalization schemes used in the two approaches [20].

The maximal values for $m_{\rm h}$ as a function of $\tan\beta$ within the $m_{\rm h}^{\rm max}$ scenario are higher by about 5 GeV than in the previous benchmark scenario. The constraints on $\tan\beta$ derived within the $m_{\rm h}^{\rm max}$ scenario are thus more conservative than the ones based on the previous scenario.

The investigation of the constraints on $\tan\beta$ that can be obtained from the experimental search limits on $m_{\rm h}$ has so far been based on the results for $m_{\rm h}$ obtained within the RG approach [5]. The recently obtained FD [8, 9] result differs from the RG result by a more complete treatment of the one-loop contributions [3] and in particular by genuine non-logarithmic two-loop terms that go beyond the leading logarithmic two-loop contributions contained in the RG result [20, 21]. Comparing the FD result (program FeynHiggs) with the RG result (program subhpole) we find that the maximal value for $m_{\rm h}$ as a function of $\tan\beta$ within the FD result is higher by up to 4 GeV.

In figure 16 we show both the effect of modifying the previous benchmark scenario to the $m_{\rm h}^{\rm max}$ scenario and the impact of the new FD two-loop result on the prediction for $m_{\rm h}$. The maximal value for the Higgs boson mass is plotted as a function of $\tan\beta$ for $m_{\rm t} = 174.3$ GeV and $M_{\rm SUSY} = 1$ TeV. The dashed curve displays the benchmark scenario, used up to now by the LEP collaborations [16]. The dotted curve shows the $m_{\rm h}^{\rm max}$ scenario. Both curves are based on the RG result (program subhpole). The solid curve corresponds to the FD result (program FeynHiggs) in the $m_{\rm h}^{\rm max}$ scenario. The increase in the maximal value for $m_{\rm h}$ by about 4 GeV from the new FD result and by a further 5 GeV if the benchmark scenario is replaced by the $m_{\rm h}^{\rm max}$ scenario has a significant effect on exclusion limits for $\tan\beta$ derived from the Higgs boson search. Combining both effects, which of course have a very different origin, the maximal Higgs boson masses are increased by almost 10 GeV compared to the previous benchmark scenario.

From the FD result we find the upper bound of $m_{\rm h} \lesssim 129$ GeV in the region of large $\tan\beta$ within the MSSM for $m_{\rm t} = 174.3$ GeV and $M_{\rm SUSY} = 1$ TeV. Higher values for $m_{\rm h}$ are obtained if the experimental uncertainty in $m_{\rm t}$ of currently $\Delta m_{\rm t} = 5.1$ GeV is taken into account and higher values are allowed for the top quark mass. As a rule of thumb, increasing $m_{\rm t}$ by 1 GeV

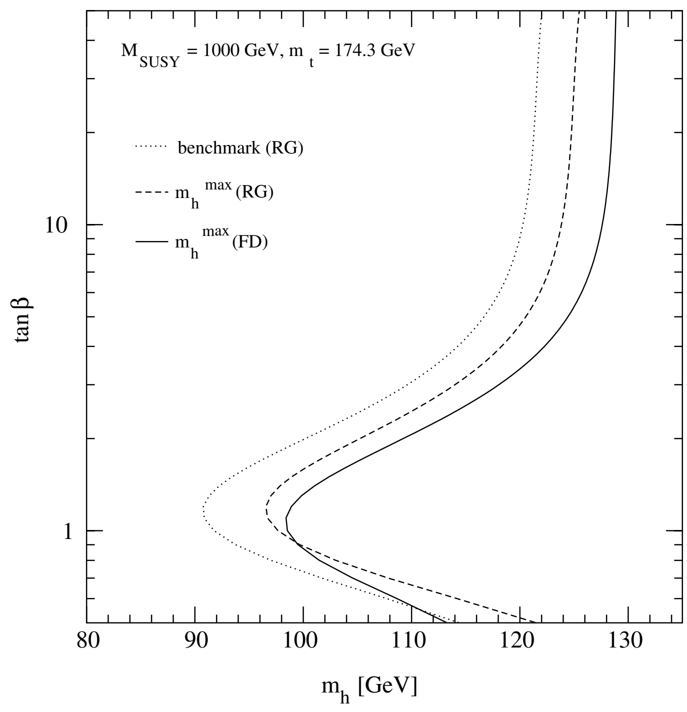

Figure 16. The upper bound on $m_{\rm h}$ is shown as a function of tan β for given $m_{\rm t}$ and $M_{\rm SUSY}$. The dashed curve displays the previous benchmark scenario. The dotted curve shows the RG result for the $m_{\rm h}^{\rm max}$ scenario, while the solid curve represents the FD result for the $m_{\rm h}^{\rm max}$ scenario.

roughly translates into an upward shift of $m_{\rm h}$ of 1 GeV. An increase of $M_{\rm SUSY}$ from 1 to 2 TeV enhances $m_{\rm h}$ by about 2 GeV in the large tan β region. As an extreme case, choosing $m_{\rm t} = 184.5$ GeV, i.e. two standard deviations above the current experimental central value, and using $M_{\rm SUSY} = 2$ TeV leads to an upper bound on $m_{\rm h}$ of $m_{\rm h} \lesssim 141$ GeV within the MSSM.

9.3. The prospective upper $m_{\rm h}$ reach of LEP

The four LEP experiments are very actively searching for the Higgs boson. Results presented recently by the LEP collaborations revealed no evidence of a SM Higgs boson signal in the data collected in 1999 at centre-of-mass energies of approximately 192, 196, 200 and 202 GeV [10–13]. From the negative results of their searches ALEPH, DELPHI and L3 have therefore individually excluded a SM Higgs boson lighter than ~101–106 Gev (at the 95% CL) [10–12].

Here we will present the expected exclusion reach of LEP assuming all the data taken by the four experiments in 1999 are combined. The ultimate exclusion reach of LEP—assuming no signal were found in the data to be collected in the year 2000—will also be estimated for several hypothetical scenarios of luminosity and centre-of-mass energy. These results are then confronted with the theoretical MSSM upper limit on $m_{\rm h}(\tan\beta)$ presented in section 9.2, in order to establish to what extent the LEP data can probe the low tan β region. We recall that models in which b–τ Yukawa coupling unification at the GUT scale is imposed favour low tan β values, tan $\beta \approx 2$, which can severely be constrained experimentally by searches at LEP. Alternatively, such models can favour tan $\beta \approx 40$, a region which however can only be partly covered at LEP.

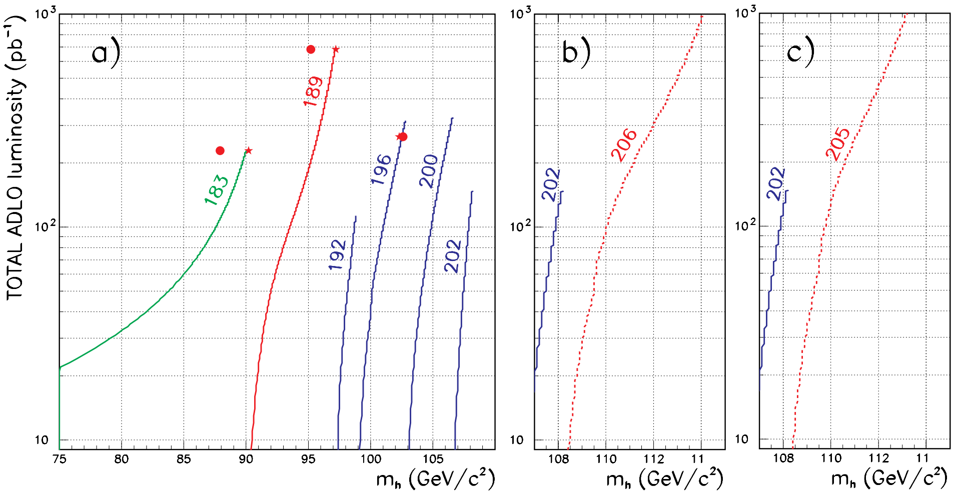

Figure 17. Predictions of the expected combined ALEPH + DELPHI + L3 + OPAL 95% CL m_h exclusion; (*a*) obtained from the data taken until the end of 1999 (solid curves). For comparison the expected (stars) and observed (dots) combined LEP limits obtained from actual data combinations [16, 24, 26] are also shown. The effect of adding to this data set new data at (*b*) $\sqrt{s} = 206$ GeV or (*c*) 205 GeV is indicated by the dashed curve.

Table 2. Summary of the total LEP data luminosity accumulated since 1997. The luminosities for the data taken in 1999 ($\sqrt{s} \geqslant 191.6$ GeV) are the (still preliminary) values quoted by the four LEP experiments at the LEPC open session [10–13].

$\sqrt{s}$ (GeV)	182.7	188.6	191.6	195.5	199.5	201.6
$\mathcal{L}$ (pb^{-1})	220.0	682.7	113.9	316.4	327.8	148.1

All experimental exclusion limits quoted in this section are implicitly meant at the 95% CL.

It has been proposed [22] that the LEP-combined expected 95% CL lower bound on m_h, m_h^{95}, for a data set consisting of data accumulated at given centre-of-mass energies, can be estimated by solving the equation

$$n(m_\mathrm{h}^{95}) = (\sigma_0 \mathcal{L}_\mathrm{eq})^\alpha, \tag{28}$$

where $n(m_\mathrm{h}^{95})$ is the number of signal events produced at the 95% CL limit. The equivalent luminosity, $\mathcal{L}_\mathrm{eq}$, is the luminosity that one would have to accumulate at the highest centre-of-mass energy in the data set in order to have the same sensitivity as in the real data set, where the data are split between several different $\sqrt{s}$ values. For a SM Higgs boson signal, the parameters σ_0 and α are $\sim$38 and $\sim$0.4 pb, respectively [22]. (These parameter values are obtained from a fit to the actual LEP-combined expected limits from $\sqrt{s} = 161$ GeV up to $\sqrt{s} = 188.6$ GeV [16,23,24].) The predicted m_h limits obtained with this method are expected to approximate the more accurate combinations done by the LEP Higgs working group, with an uncertainty of the order of ± 0.3 GeV.

Solving equation (28) for the existing LEP data with 183 GeV $\lesssim \sqrt{s} \lesssim 202$ GeV (table 2) results in a predicted combined exclusion of $m_\mathrm{h} < 108.2$ GeV for the SM Higgs boson (see figure 17(*a*)).

Based on the current LEP operational experience, it is believed that in the year 2000 stable running is possible up to $\sqrt{s} = 206$ GeV [25]. Figure 17(*b*) demonstrates the impact

Table 3. Predictions of the sensitivity of the four LEP experiments combined, for several hypothetical data sets. The table shows the expected excluded SM Higgs boson mass (m_{h}^{95}, in GeV) as well as the corresponding excluded $\tan\beta$ region in the $m_{\mathrm{h}}^{\max}$ benchmark scenario (with $m_{\mathrm{t}} = 174.3$ GeV, $M_{\mathrm{SUSY}} = 1$ TeV), when new data at the indicated $\sqrt{s}$ are combined with the existing data set (table 2). The luminosities indicated are for the four LEP experiments combined. The results shown are valid only if no signal were found in the data. (Note that, as it is not foreseen at the moment that it will be possible to run LEP at $\sqrt{s} > 206$ GeV, scenario (8) is probably unrealistic.)

$\sqrt{s}$ (GeV)	204	205	206	208	m_{h}^{95}	$\tan\beta^{95}$
(1) $\mathcal{L}$ (pb^{-1})	—	—	100	—	110.0	0.6–2.1
(2) $\mathcal{L}$ (pb^{-1})	—	—	500	—	113.0	0.5–2.4
(3) $\mathcal{L}$ (pb^{-1})	—	—	1000	—	114.1	0.5–2.5
(4) $\mathcal{L}$ (pb^{-1})	—	120	—	—	110.0	0.6–2.1
(5) $\mathcal{L}$ (pb^{-1})	—	840	—	—	113.0	0.5–2.4
(6) $\mathcal{L}$ (pb^{-1})	100	100	400	—	113.1	0.5–2.4
(7) $\mathcal{L}$ (pb^{-1})	150	300	300	—	113.3	0.5–2.4
(8) $\mathcal{L}$ (pb^{-1})	150	300	300	280	115.0	0.5–2.6

of additional data collected at $\sqrt{s} = 206$ GeV on the exclusion. For instance, if no evidence of a signal were found in the data, collecting 500 (1000) pb^{-1} at this centre-of-mass energy would increase the m_{h} limit to 113.0 (114.1) GeV. Figure 17(*c*) shows the degradation in the sensitivity to a Higgs boson signal if the data in the year 2000 were accumulated at $\sqrt{s} = 205$ GeV instead: in this case the luminosity required to exclude up to $m_{\mathrm{h}} = 113$ GeV would be 840 pb^{-1}.

In table 3 the expected SM Higgs boson limit is shown for several possible LEP running scenarios in the year 2000. Taking into account that the *experimental* MSSM m_{h} exclusion in the range $0.5 \lesssim \tan\beta \lesssim 3$ is (i) essentially independent of $\tan\beta$ and (ii) equal in value to the SM m_{h} exclusion (see, e.g., [24,26]), m_{h}^{95} can be converted into an excluded $\tan\beta$ range in the $m_{\mathrm{h}}^{\max}$ benchmark scenario described in section 9.2. This is done by intersecting the experimental exclusion and the solid curve in figure 16. Using the LEP data taken until the end of 1999 (for which $m_{\mathrm{h}}^{95} = 108.2$ GeV) one can already expect to exclude $0.6 \lesssim \tan\beta \lesssim 1.9$ within the MSSM for $m_{\mathrm{t}} = 174.3$ GeV and $M_{\mathrm{SUSY}} = 1$ TeV. Note that in determining the excluded $\tan\beta$ regions in table 3 the theoretical uncertainty from unknown higher-order corrections has been neglected. As can be seen from table 3, several plausible scenarios for adding new data at higher energies can extend the exclusion to $m_{\mathrm{h}} \lesssim 113$ GeV ($0.5 \lesssim \tan\beta \lesssim 2.4$).

9.4. The upper limit on m_{h} in the mSUGRA scenario

The mSUGRA scenario is described by four independent parameters and a sign, namely the common squark mass M_0, the common gaugino mass $M_{1/2}$, the common trilinear coupling A_0, $\tan\beta$ and the sign of μ. The universal parameters are fixed at the GUT scale, where we assumed unification of the gauge couplings. Then they are run down to the electroweak scale with the help of RG equations [4, 15, 27–32]. The condition of REWSB puts an upper bound on M_0 of about $M_0 \lesssim 5$ TeV (depending on the values of the other four parameters).

In order to obtain a precise prediction for m_{h} within the mSUGRA scenario, we employ the complete two-loop RG running with appropriate thresholds (both logarithmic and finite for the gauge couplings and using the so-called θ-function approximation for the masses [15]) including full one-loop minimization conditions for the effective potential, in order to extract all the parameters of the mSUGRA scenario at the EW scale. This method has been

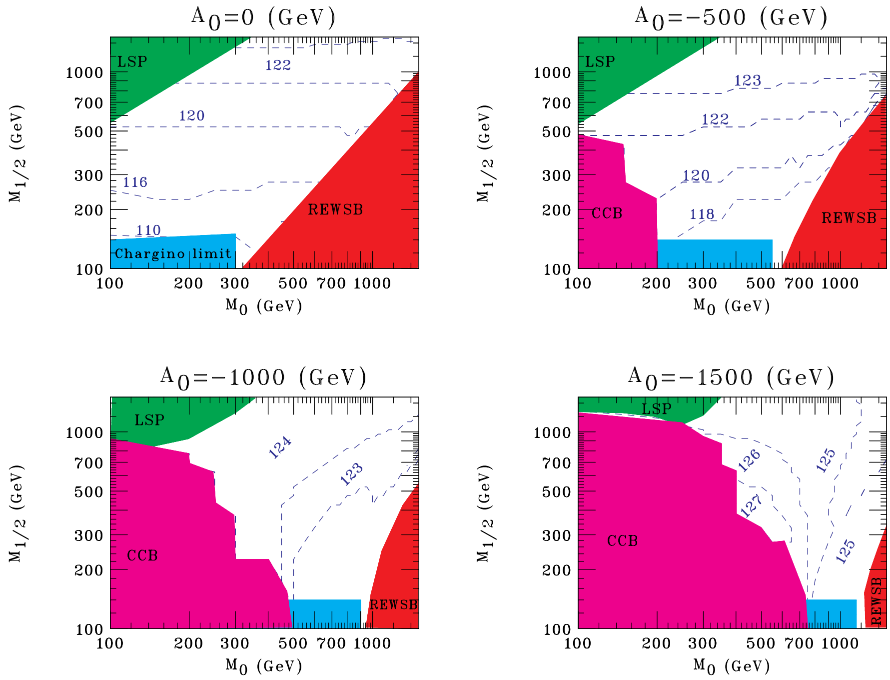

Figure 18. In the M_0–$M_{1/2}$ plane the contour lines of m_h are shown for four values of A_0. The numbers refer to m_h in the respective region within ±0.5 GeV. The regions that are excluded by REWSB, the CCB or LSP conditions, or by direct chargino search are also indicated.

combined with the presently most precise result of m_h based on a FD calculation [8, 9]. This has been carried out by combining the codes of two programs, namely SUITY [33] and FeynHiggs [19].

In order to investigate the upper limit on the Higgs boson mass in the mSUGRA scenario, we keep $\tan\beta$ fixed at a large value, $\tan\beta = 30$. Concerning the sign of the Higgs mixing parameter, μ, we find larger m_h values (compatible with the constraints discussed below) for negative μ (in the convention of (26)). In the following we analysed the upper limit on m_h as a function of the other mSUGRA parameters, M_0, $M_{1/2}$ and A_0. Our results are displayed in figure 18 for four values of A_0: $A_0 = 0, -500, -1000, -1500$ GeV. We show contour lines of m_h in the M_0–$M_{1/2}$-plane. The numbers inside the plots indicate the lightest Higgs boson mass in the respective area within ±0.5 GeV. The upper bound on the lightest $\mathcal{CP}$-even Higgs boson mass is found to be at most 127 GeV. This upper limit is reached for $M_0 \approx 500$ GeV, $M_{1/2} \approx 400$ GeV and $A_0 = -1500$ GeV. Concerning the analysis the following should be noted:

- We have chosen the current experimental central value for the top quark mass, $m_t = 174.3$ GeV. As mentioned above, increasing m_t by 1 GeV results in an increase of m_h of approximately 1 GeV.
- The mSUGRA parameters are taken to be real, no SUSY $\mathcal{CP}$-violating phases are assumed.
- We have chosen negative values for the trilinear coupling, because m_h turns out to be increased by going from positive to negative values of A_0. $|A_0|$ is restricted from above by the condition that no negative squares of squark masses and no charge or colour breaking minima appear.

- The regions in the M_0–$M_{1/2}$-plane that are excluded for the following reasons are also indicated:
  - ∗ REWSB: parameter sets that do not fulfil the REWSB condition.
  - ∗ CCB: regions where charge or colour breaking minima occur or negative squared squark masses are obtained at the EW scale.
  - ∗ LSP: sets where the lightest neutralino is not the LSP. Mostly there the lightest scalar tau becomes the LSP.
  - ∗ Chargino limit: parameter sets which correspond to a chargino mass that is already excluded by direct searches.
- We do not take into account the $b \to s\gamma$ constraint as the authors of [34, 35] do. This could reduce the upper limit but still the experimental and theoretical uncertainties of this constraint are quite large.

9.5. Conclusions

We have analysed the upper bound on m_h within the MSSM. Using the FD result for m_h, which contains new genuine two-loop corrections, leads to an increase of m_h of up to 4 GeV compared with the previous result obtained by RG methods. We have furthermore investigated the MSSM parameters for which the maximal m_h values are obtained and have compared the m_h^{max} scenario with the previous benchmark scenario. For $m_t = 174.3$ GeV and $M_{SUSY} = 1$ TeV we find $m_h \lesssim 129$ GeV as upper bound in the MSSM. In the case that no evidence of a Higgs signal is found before the end of running in 2000, experimental searches for the Higgs boson at LEP can ultimately be reasonably expected to exclude $m_h \lesssim 113$ GeV. In the context of the m_h^{max} benchmark scenario (with $m_t = 174.3$ GeV, $M_{SUSY} = 1$ TeV) this rules out the interval $0.5 \lesssim \tan\beta \lesssim 2.4$ at the 95% CL within the MSSM. Within the mSUGRA scenario, the upper bound on m_h is found to be $m_h \lesssim 127$ GeV for $m_t = 174.3$ GeV. This upper limit is reached for the mSUGRA parameters $M_0 \approx 500$ GeV, $M_{1/2} \approx 400$ GeV and $A_0 = -1500$ GeV. The upper bound within the mSUGRA scenario is lower by 2 and 4 GeV than the bound obtained in the general MSSM for $M_{SUSY} = 1$ TeV and $M_{SUSY} = 2$ TeV, respectively.

Acknowledgments

AD acknowledges financial support from the Marie Curie Research Training Grant ERB-FMBI-CT98-3438. AD would also like to thank Ben Allanach for useful discussions. PTD would like to thank Jennifer Kile for providing the SM Higgs boson production cross sections. GW thanks C E M Wagner for useful discussions.

References

[1] Haber H and Hempfling R 1991 *Phys. Rev. Lett.* **66** 1815
Ellis J, Ridolfi G and Zwirner F 1991 *Phys. Lett.* B **257** 83
Ellis J, Ridolfi G and Zwirner F 1991 *Phys. Lett.* B **262** 477
[2] Chankowski P, Pokorski S and Rosiek J 1994 *Nucl. Phys.* B **423** 437
[3] Dabelstein A 1995 *Nucl. Phys.* B **456** 25
(Dabelstein A 1995 *Preprint* hep-ph/9503443)
Dabelstein A 1995 *Z. Phys.* C **67** 495
(Dabelstein A 1995 *Preprint* hep-ph/9409375)
[4] Bagger J, Matchev K, Pierce D and Zhang R 1997 *Nucl. Phys.* B **491** 3
(Bagger J, Matchev K, Pierce D and Zhang R 1996 *Preprint* hep-ph/9606211)
[5] Carena M, Espinosa J, Quirós M and Wagner C 1995 *Phys. Lett.* B **355** 209
(Carena M, Espinosa J, Quirós M and Wagner C 1995 *Preprint* hep-ph/9504316)

Carena M, Quirós M and Wagner C 1996 *Nucl. Phys.* B **461** 407
(Carena M, Quirós M and Wagner C 1995 *Preprint* hep-ph/9508343)
[6] Haber H, Hempfling R and Hoang A 1997 *Z. Phys.* C **75** 539
(Haber H, Hempfling R and Hoang A 1996 *Preprint* hep-ph/9609331)
[7] Hempfling R and Hoang A 1994 *Phys. Lett.* B **331** 99
(Hempfling R and Hoang A 1994 *Preprint* hep-ph/9401219)
Zhang R-J 1999 *Phys. Lett.* B **447** 89
(Zhang R-J 1998 *Preprint* hep-ph/9808299)
[8] Heinemeyer S, Hollik W and Weiglein G 1998 *Phys. Rev.* D **58** 091701
(Heinemeyer S, Hollik W and Weiglein G 1998 *Preprint* hep-ph/9803277)
Heinemeyer S, Hollik W and Weiglein G 1998 *Phys. Lett.* B **440** 296
(Heinemeyer S, Hollik W and Weiglein G 1998 *Preprint* hep-ph/9807423)
[9] Heinemeyer S, Hollik W and Weiglein G 1999 *Eur. Phys. J.* C **9** 343
(Heinemeyer S, Hollik W and Weiglein G 1998 *Preprint* hep-ph/9812472)
[10] Blondel A (ALEPH Collaboration) Talk *LEPC Meeting (Nov. 1999)*
[11] J. Marco (DELPHI Collaboration) Talk *LEPC meeting (Nov. 1999)*
[12] Rahal-Callot G (L3 Collaboration) Talk *LEPC meeting (Nov. 1999)*
[13] Ward P (OPAL Collaboration) Talk *LEPC meeting (Nov. 1999)*
[14] Ibañez L E and Ross G G 1982 *Phys. Lett.* **110** 215
Inoue K, Kakuto A, Komatsu H and Takeshita S 1982 **68** 927
Inoue K, Kakuto A, Komatsu H and Takeshita S 1984 *Prog. Theor. Phys.* **71** 96
Ellis J, Nanopoulos D V and Tamvakis K 1983 *Phys. Lett.* B **121** 123
Ibañez L E 1983 *Nucl. Phys.* B **218** 514
Alvarez-Gaumé L, Polchinski J and Wise M 1983 *Nucl. Phys.* B **221** 495
Ellis J, Hagelin J S, Nanopoulos D V and Tamvakis K 1983 *Phys. Lett.* B **125** 275
Alvarez-Gaumé L, Claudson M and Wise M 1982 *Nucl. Phys.* B **207** 96
[15] Dedes A, Lahanas A B and Tamvakis K 1996 *Phys. Rev.* D **53** 3793
(Dedes A, Lahanas A B and Tamvakis K 1995 *Preprint* hep-ph/9504239)
[16] The LEP working group for Higgs boson searches CERN-EP/99-060
[17] Heinemeyer S, Hollik W and Weiglein G 1999 DESY 99-120 *Preprint* hep-ph/9909540
[18] Carena M, Heinemeyer S, Wagner C and Weiglein G 1999 *Preprint* hep-ph/9912223
[19] Heinemeyer S, Hollik W and Weiglein G 2000 *Comput. Phys. Commun.* **124** 76
[20] Carena M, Haber H, Heinemeyer S, Hollik W, Wagner C and Weiglein G 2000 *Preprint* hep-ph/0001002
[21] Heinemeyer S, Hollik W and Weiglein G 1999 *Phys. Lett.* B **455** 179
(Heinemeyer S, Hollik W and Weiglein G 1999 *Preprint* hep-ph/9903404)
(Heinemeyer S, Hollik W and Weiglein G 1999 *Preprint* hep-ph/9910283)
[22] Janot P 1999 How should we organize the Higgs safari? *Proc. 9th Chamonix SPS and LEP Performance Workshop (Jan. 1999)* ed J Poole CERN-SL-99-007-DI
[23] The LEP working group for Higgs boson searches CERN-EP/98-046
[24] The LEP working group for Higgs boson searches Paper #6_49 *Int. Europhys. Conf. on High Energy Physics (Tampere, Finland, July 1999)* ALEPH 99-081, DELPHI 99-142, L3 note 2442, OPAL TN-614
[25] Butterworth A Talk *LEPC meeting (Nov. 1999)*
[26] McNamara P 1999 Combined LEP Higgs search results up to $\sqrt{s}$ =196 GeV Talk *LEPC meeting (Sept. 1999)*
[27] Ross G G and Roberts R G 1992 *Nucl. Phys.* B **377** 571
[28] Nath P and Arnowitt R 1992 *Phys. Lett.* B **287** 89
[29] Faraggi A and Grinstein B 1994 *Nucl. Phys.* B **422** 3
[30] Castano D J, Piard E J and Ramond P 1994 *Phys. Rev.* D **49** 4882
(Castano D J, Piard E J and Ramond P 1993 *Preprint* hep-ph/9308335)
[31] Barger V, Berger M S and Ohmann P 1994 *Phys. Rev.* D **49** 4908
(Barger V, Berger M S and Ohmann P 1993 *Preprint* hep-ph/9311269)
[32] Kane G L, Kolda C, Roszkowski L and Wells J D 1994 *Phys. Rev.* D **49** 6173
(Kane G L, Kolda C, Roszkowski L and Wells J D 1993 *Preprint* hep-ph/9312272)
[33] Dedes A, Lahanas A B, Spanos V and Tamvakis K SUITY: A program for the minimal SUpergravITY spectrum in preparation
[34] Matchev K and Pierce D 1999 *Phys. Lett.* B **445** 331
[35] de Boer W, Grimm H J, Gladyshev A V and Kazakov D I 1998 *Phys. Lett.* B **438** 281
de Boer W Talk *ECFA/DESY Linear Collider Workshop (Obernai, Oct. 1999)*

10. An update of the program HDECAY

A Djouadi, J Kalinowski and M Spira

Abstract. The program HDECAY determines the decay widths and branching ratios of the Higgs bosons within the SM and its minimal SUSY extension, including the dominant higher-order corrections. New theoretical developments are briefly discussed and the new ingredients incorporated in the program are summarized.

The search strategies for Higgs bosons at LEP, Tevatron, LHC and future e^+e^- linear colliders (LC) exploit various Higgs boson decay channels. The strategies depend not only on the experimental setup (hadron versus lepton colliders) but also on the theoretical scenarios: the SM or some of its extensions such as the minimal supersymmetric standard model (MSSM). It is of vital importance to have reliable predictions for the branching ratios of the Higgs boson decays for these theoretical models.

The current version of the program HDECAY [1] can be used to calculate Higgs boson partial decay widths and branching ratios within the SM and the MSSM and includes:

- All decay channels that are kinematically allowed and which have branching ratios larger than 10^{-4}, including the loop-mediated, the three-body decay modes and (in the MSSM) the cascade and the SUSY decay channels [2].
- All relevant higher-order QCD corrections to the decays into quark pairs and to the loop-mediated decays into gluons are incorporated in a complete form [3]; the small leading electroweak corrections are also included.
- Double off-shell decays of the CP-even Higgs bosons into massive gauge bosons which then decay into four massless fermions, and all important below-threshold three-body decays [4].
- In the MSSM, the complete radiative corrections in the effective potential approach with full mixing in the stop/sbottom sectors; it uses the RG improved values of the Higgs masses and couplings and the relevant next-to-leading-order corrections are implemented [5].
- In the MSSM, all the decays into SUSY particles (neutralinos, charginos, sleptons and squarks including mixing in the stop, sbottom and stau sectors) when they are kinematically allowed [6]. The SUSY particles are also included in the loop-mediated $\gamma\gamma$ and gg decay channels.

The source code of the program, written in FORTRAN, has been tested on computers running under different operating systems. The program provides a very flexible and convenient usage, fitting to all options of phenomenological relevance. The basic input parameters, fermion and gauge boson masses and their total widths, coupling constants and, in the MSSM, soft SUSY-breaking parameters can be chosen from an input file. In this file several flags allow switching on/off or changing some options (e.g. choosing a particular Higgs boson, including/excluding the multi-body or SUSY decays, or including/excluding specific higher-order QCD corrections).

Since the release of the original version of the program several bugs have been fixed and a number of improvements and new theoretical calculations have been implemented. The following points have recently been made:

- Link to the FeynHiggsFast routine for Higgs masses and couplings [7].
- Link to the SUSPECT routine for RG evolution of SUGRA parameters [8].

- Implementation of Higgs boson decays to gravitino + gaugino [9].
- Inclusion of gluino loops in Higgs decays to $b\bar{b}$ [10].
- Inclusion of QCD corrections in Higgs decays to squarks [11].
- Determination and inclusion of the RG-improved two-loop contributions to the MSSM Higgs self-interactions.

The logbook of all modifications and the most recent version of the program can be found in [12].

Acknowledgments

JK has been supported in part by the KBN grant No 2 P03B 030 14 and the Foundation for Polish–German Collaboration grant No 3310/97/LN. We thank Peter Zerwas for continuous interest and support.

References

[1] Djouadi A, Kalinowski J and Spira M 1998 *Comput. Phys. Commun.* **108** 56
[2] Spira M 1998 *Fortschr. Phys.* **46** 203
[3] Djouadi A, Spira M and Zerwas P M 1996 *Z. Phys.* C **70** 427
[4] Djouadi A, Kalinowski J and Zerwas P M 1996 *Z. Phys.* C **70** 435
[5] Carena M, Quiros M and Wagner C E M 1996 *Nucl. Phys.* B **461** 407
Haber H E, Hempfling R and Hoang A H 1997 *Z. Phys.* C **75** 539
Heinemeyer S, Hollik W and Weiglein G 1998 *Phys. Rev.* D **58** 091701
[6] Djouadi A, Kalinowski J and Zerwas P M1993 *Z. Phys.* C **C57** 569
Djouadi A, Janot P, Kalinowski J and Zerwas P M 1996 *Phys. Lett.* B **376** 220
Djouadi A, Kalinowski J, Ohmann P and Zerwas P M 1997 *Z. Phys.* C **74** 93
[7] Heinemeyer S, Hollik W and Weiglein G 2000 *Comput. Phys. Commun.* **124** 76
(Heinemeyer S, Hollik W and Weiglein G 2000 *Preprint* hep-ph/0002213)
[8] Djouadi A, Kneur J L and Moultaka G 1999 *Preprint* hep-ph/9901246
[9] Djouadi A and Drees M 1997 *Phys. Lett.* B **407** 243
[10] Dabelstein A 1995 *Nucl. Phys.* B **456** 25
Jiménez R A and Solà J 1996 *Phys. Lett.* B **389** 53
Coarasa J A, Jiménez R A and Solà J 1996 *Phys. Lett.* B **389** 312
[11] Bartl A, Eberl H, Hidaka K, Kon T, Majerotto W and Yamada Y 1997 *Phys. Lett.* B **402** 303
Arhrib A, Djouadi A, Hollik W and Jünger C 1998 *Phys. Rev.* D **57** 5860
[12] http://www.desy.de/∼spira/prog